UNIVERSITY OF BIRMINGHAM

THE ROLE OF mTOR SIGNALLING IN RGC AXON REGENERATION

THE ROLE OF Fn14 AND TWEAK IN THE DEVELOPMENT AND RESOLUTION OF LIVER FIBROSIS

by

Annika Wilhelm

College of Medical and Dental Sciences
University of Birmingham
August 2011

UNIVERSITY OF BIRMINGHAM

THE ROLE OF mTOR SIGNALLING IN RGC AXON REGENERATION

by

Annika Wilhelm

A thesis submitted to the University of Birmingham in partial fulfilment of the requirements for the award of the Master of Research

Neuropharmacology and Neurobiology Section
School of Clinical and Experimental Medicine
College of Medical and Dental Sciences
University of Birmingham
August 2011

ABSTRACT

Axons from the central nervous system (CNS) do not regenerate, causing a major problem for recovery after CNS injury. One possible reason why axon growth is inhibited is intracellular suppression of growth signals. In this work, we examined the role of RTP801 during axon regeneration *in vitro* and *in vivo*. RTP801 is an upstream inhibitor of mTOR signalling, which is central to cell growth. We report here that retinal ganglion cells (RGC) *in vitro* and *in vivo* responded to siRNA designed against RTP801 (siRTP801). Due to a limited amount of time not all experiments could be repeated in triplicate however a trend shows that siRTP801 treatment does not enhance RGC survival or neurite outgrowth *in vitro* but increases neurite length. Treatment with siRTP801 in combination with ciliary neurotrophic factor (CNTF) and an anti-apoptotic caspase-2 inhibitor seems to be most effective in promoting long RGC neurites. The *in vitro* results support the data from the *in vivo* work where an increase of long distant axons has been documented. However, the generated data is not conclusive and more experiments need to be carried out. Nevertheless, these findings demonstrate a potential for siRTP801 as a novel strategy to enhance axon regeneration in RGC.

ACKNOWLEDGEMENTS

I am most grateful to my principal supervisor Prof Ann Logan for her great advice and support throughout my project and my second supervisor Dr Zubair Ahmed for his guidance and knowledge about RGC axon regeneration. Without them it would not have been possible to complete this project. I owe my deepest gratitude to Prof Martin Berry who performed all surgical procedures.

Amongst my fellow postgraduate students I would like to thank Jenna O'Neil for her academic and moral support. I would also like to thank the rest of the Molecular Neuroscience Research Group.

TABLE OF CONTENTS

1. INTRODUCTION

1.1 Axon Regeneration in the CNS after Injury

Compared to the peripheral nervous system (PNS), axon regeneration of the central nervous system (CNS) in mature mammals is very limited. Trauma to the neuronal network of the CNS caused by factors, such as a stroke, brain and spinal cord injury or specific neurodegenerative diseases, leaves people suffering from irreversible neurological deficits. The reason for that is that injured CNS neurons exhibit an immediate axonal growth response, but this response ceases quickly and the original axon connections cannot be re-established (1). The knowledge about the pathophysiological process of CNS injury is still insufficient and therefore limits the discovery of novel treatments that will effectively induce axon growth. Hence it is necessary to gain a greater understanding of the underpinning mechanisms of the pathophysiology in order to discover more effective treatments and prevent long-term disability in patients suffering from CNS injury.

1.2 The Visual System to Study CNS Regeneration

Optic nerve (ON) injury is a good model in which to carry out research on CNS axon regeneration. Its structure is simple, with well-defined axon projections and it is relatively easy to access as it lies outside the cranium. The CNS axonal population that constitute the ON derive from the retinal ganglion cells (RGC).

RGC are present in the innermost layer of the retina of the eye where they receive information from the underlying retinal photoreceptors and relay them to the brain. The ON, which is made up of only RGC axons and their supporting cells, begins at the optic disk where RGC axons leave the orbit. It decussates with the ON of the other eye at the optic chiasm. From there the axons form the optic tracts, that will terminate in the lateral geniculate body, superior colliculus and the pretectal area of the brain to send information on to the visual neocortex and other areas.

1.3 Strategies to Promote RGC Axon Regeneration

1.3.1 Apoptotic Pathway

RGC begin to undergo apoptosis approximately 5 days after axon injury if the ON is damaged intraorbitally at a gap of about 0.5mm from the eye. After two weeks around 90% of the RGC will have died (2).

Apoptosis of RGC can be inhibited in several ways. One way to prevent apoptosis of RGC is to inhibit the intracellular signalling caspases. Caspase-2, for example, is evolutionary the most highly conserved caspase and functions both as an initiator and effector caspase (3). Levels of active caspase-2 are elevated after ON injury and inhibiting caspase-2 with a synthetic siRNA significantly increases RGC survival for 30 days post ON injury (4). This indicates a great neuroprotective potential of caspase-2 inhibitors. Another caspase inhibitor, benzyloxycarbonyl-Asp-Glu-Val-Asp-chloromethylketone, that inhibits caspase-3, was also demonstrated to delay RGC death (5). However, caspase-3 is an effector caspase and relies on activation by initiator caspases. It

would seem sensible to target initiator caspases rather than effector caspases that have less influence in preventing apoptosis. Overexpression of the anti-apoptotic protein Bcl-2 after ON injury is also a way of preventing RGC apoptosis and this allows most of the RGC to survive for a long time post axotomy (6,7). However, in general the number of surviving RGC and the time of onset of apoptosis depend on the distance between the eye and the site of axonal injury. So, an injury close to the eye will cause a more rapid and extensive RGC death than an injury that is located further away from the eye (8).

1.3.2 Cell Extrinsic Inhibitors of Axon Growth

Although it is important that RGC do not die after injury it is crucial for CNS regeneration that the axotomized RGC start to grow axons again to re-connect with their corresponding counterparts. Elements in the extracellular environment of the CNS suppress axon growth, in particular those derived from myelin (9), the meningoglial scar (10) and the perineuronal net (11). RGC axons are covered in myelin that is produced by oligodendrocytes. It forms a sheath around the axons to increase the speed of nerve impulse conduction. Myelin-derived proteins that act as axon growth inhibitory molecules include Nogo-A (12), myelin-associated glycoprotein (MAG) (13) and oligodendrocyte-myelin glycoprotein (OMgp) (14) (Figure 1). These proteins bind to the Nogo receptor complex that consists of NgR1, Lingo-1 (15) and p75NTR (16) or TAJ/TROY (17). This interaction leads to inhibition of axon growth by inducing growth cone collapse *via* the RhoA pathway (14,18) (Figure 1). In addition, other receptors and ligands of myelin-derived proteins involved in inhibition of axon growth such as leucine-rich, glioma-inactivated (LGI) gene product (19) and G-protein-

coupled receptor 50 (GPR50) (20) have been recently identified. The meningioglial scar that generally forms after CNS injury is considered as both a physical and biochemical barrier of axon growth (10). Within the scar and the perineuronal net are proteoglycans that are major inhibitors of axon growth (21). Proteoglycans, such as chondroitin sulphate proteoglycans (CSPG), directly interact with receptor protein tyrosine phosphatase σ (RPTPσ) to signal axonal growth inhibition by the same RhoA-signalling cascade (22).

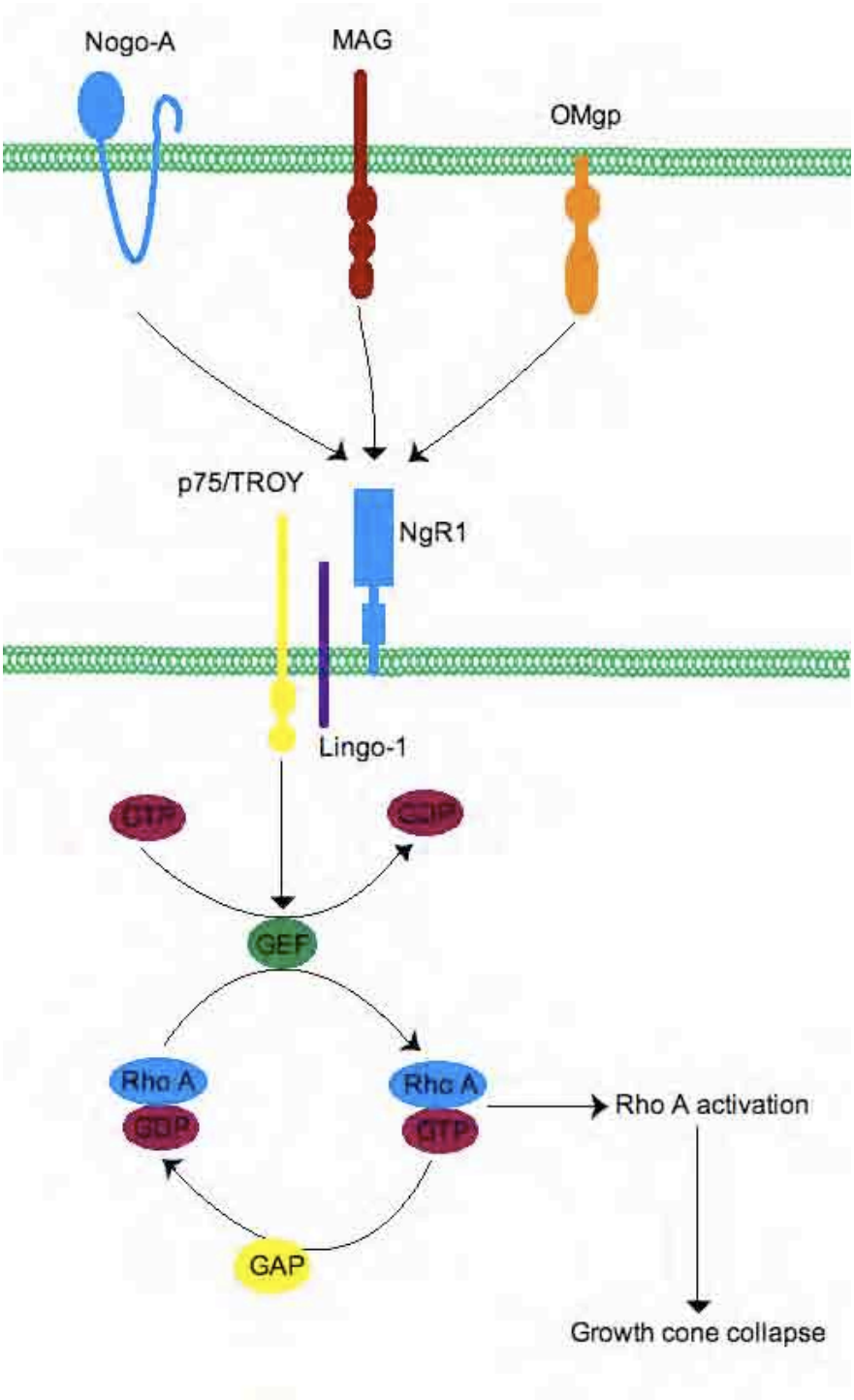

Fig 1. Nogo-A, myelin-associated glycoprotein (MAG) and oligodendrocyte-myelin glycoprotein (OMgp) interact with the Nogo receptor complex consisting of NgR1, Lingo-1 and p75NTR or TROY to signal neurite outgrowth inhibition. The signal is send into the cell *via* p75NTR or TROY to convert the inactive form of RhoA into the active form. Activation of RhoA triggers numerous downstream events that eventually lead to growth cone collapse.

Several strategies to overcome axon growth inhibition have been investigated, such as expressing a dominant-negative form of the Nogo receptor. However, supressing the receptor did not show beneficial effects without coincident stimulation of axon growth (23). In addition, other research has demonstrated that counteracting inhibition is not enough to stimulate extensive axon regeneration (24). One reason for that might be that, even when a few inhibitors are knocked out, others will still be functioning and inhibiting axon regeneration. Another reason might be that the low intrinsic growth potential of CNS neurons still restrict axon regeneration even if all inhibitory factors can be overcome.

1.3.3 Growth Potential of RGC

As the PNS is capable of axon regeneration, research has been carried out with peripheral nerve grafts implanted into the vitreous body of the eye to identify key regeneration factors. The grafts led to expression of growth-associated protein GAP-43 in RGC (25) and even enabled regeneration of axons through the ON (26). The PNS graft contained Schwann cells and numerous macrophages as a result of leaving the graft *in situ* for a week before transplantation. Factors secreted by Schwann cells or macrophages could have been responsible of the excessive axon outgrowth.

An equal amount of axon regeneration from RGC after ON injury was detected by simply injuring the lens (27,28). Leon *et al.* discovered that the lens injury was accompanied by an influx of activated blood borne macrophages into the eye (27). Intravitreal injections of a pro-inflammatory agent called Zymosan generated even stronger axon regeneration than a peripheral nerve graft or lens injury (27,29). These results suggest that macrophage-derived factors can play

a key role in promoting axon regeneration in the CNS. The macrophage-derived growth factor that was involved in RGC axon regeneration was identified to be oncomodulin (30,31). Oncomodulin binds to a RGC cell surface receptor with high affinity and specificity. When oncomodulin in addition to cAMP was intravitreally injected, axon regeneration was almost as extensive as that seen with injection of macrophages (30). cAMP on its own, however, had little effect on axon regeneration, which indicates that cAMP's effect on axon regeneration is mediated by oncomodulin (32).

Administration of the ciliary neurotrophic factor (CNTF) also led to RGC axon regeneration and increased RGC survival (33). Moreover, a combination of other neurotrophic factors delivered intravitreally induced robust regeneration of RGC axons after injury (34). This suggests that axons need to overcome a signalling threshold in order to grow and that there is a final common pathway that induces growth.

1.4 PTEN/mTOR Pathway

Most of these above named growth stimulatory factors activate mTOR. An alternative way to generate RGC axon regeneration is by directly modulating the PTEN/mTOR pathway. This pathway regulates cell growth by modulating protein synthesis and its perturbation is associated with numerous diseases, such as Peutz-Jegher's syndrome, tuberous sclerosis complex (TSC) and cancer (35). This pathway is triggered by activation of receptor tyrosine kinases, including Trk receptors, which activate phosphoinositide 3-kinases (PI3K)

(Figure 2). PI3K converts phosphatidylinositol 4,5-bisphosphate (PIP_2) into phosphatidylinositol 3,4,5-trisphosphate (PIP_3). PIP_3 then recruits and activates phosphatidylinositol-dependent kinase 1/2 (PDK1/2) that leads to activation of Akt. Tuberous sclerosis complex (TSC) 1 and 2 form a complex to inhibit mammalian target of rapamycin (mTOR) (36). However, Akt activation results in phosphorylation and inhibition of TSC2 that prevents the TSC complex from supressing mTOR activation *via* Ras homolog enriched in brain (Rheb) (37). mTOR then phosphorylates and activates its substrates, eukaryote initiation factor 4E-binding protein 1 (4E-BP1) and ribosomal protein S6 kinase 1 (S6K1) that lead to stimulation of protein synthesis (Figure 2).

Negative regulators of this pathway are phosphatase and tensin homolog (PTEN), RTP801 (also known as Redd1) and, as described above, TSC1/2. PTEN inhibits this pathway by antagonising PI3K when catalysing the change from PIP_3 to PIP_2 (38). RTP801 blocks activation of mTOR by modulating the activity of the TSC1/2 complex (39). So, if PTEN, RTP801 or TSC are active they hinder protein synthesis and therefore reduce cell growth (Figure 2). Therefore, these proteins may be suitable targets for inhibition in order to activate mTOR and stimulate disinhibited RGC axon growth in the ON.

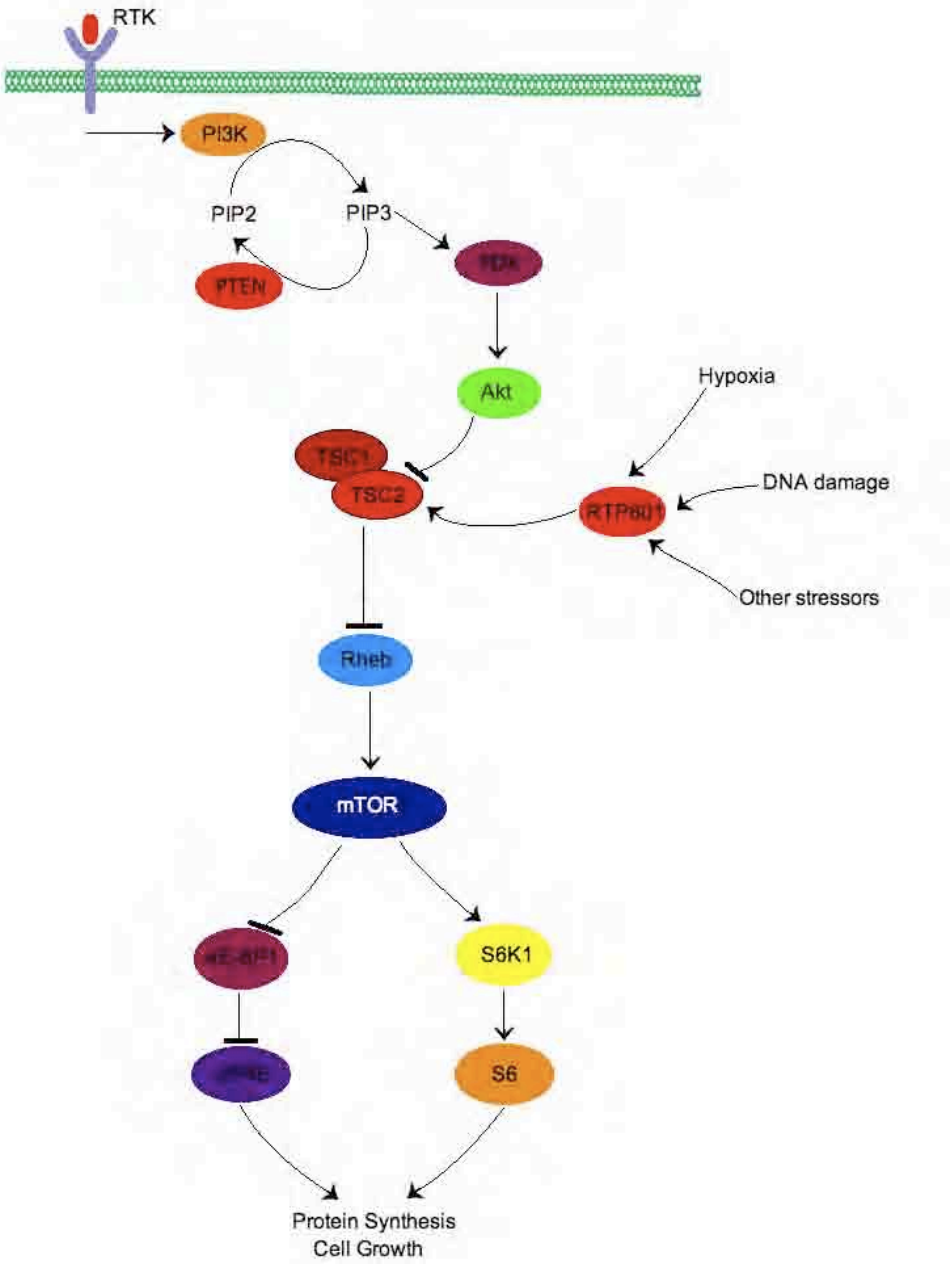

Fig 2. The PTEN/mTOR pathway regulates cell growth by modulating protein synthesis. The pathway is triggered by activation of PI3K *via* receptor tyrosine kinase (RTK). PI3K converts PIP2 to PIP3. This step is antagonised by PTEN. PIP3 recruits PDK that will activate Akt. Akt can then inhibit TSC, an inhibitor of mTOR. When mTOR is active it phosphorylates its substrates to induce protein synthesis. RTP801 is a protein that is activated by stressors such as DNA damage and hypoxia. It positively modulates the activity of TSC to prevent protein synthesis.

1.5 mTOR/PTEN Pathway in RGC Axon Regeneration

1.5.1 mTOR Activation

When mTOR is active it phosphorylates a number of different substrates that result in protein translation and ribosome biogenesis (40). In adult RGC, active mTOR levels are highly reduced compared to those in embryonic neurons. In addition, RGC axotomy reduces the levels of active mTOR even further. Deleting PTEN which is, as mentioned above, an upstream inhibitor of mTOR results in raised levels of phosphorylated S6 and axon regeneration. When rapamycin, an inhibitor of mTOR, is administered into PTEN-deleted mice, RGC axon regeneration is largely abolished (41). These results indicate that mTOR is a key component of axon regeneration in the CNS.

1.5.2 Inhibiting PTEN

Inhibition of PTEN leads to accumulation of PIP_3 and eventually to activation of Akt, which in turn inhibits TSC and activates mTOR. Conditional deletions of PTEN and several other growth control genes such as, Rb and p53, were performed and RGC survival and axon regeneration were monitored. PTEN exhibited the strongest effect on RGC survival and axon regeneration out of the tested growth genes (41). Combining intraocular inflammation, cAMP elevation and deletion of PTEN resulted in the best so far documented long-distance RGC axon regeneration. In fact this specific combination increased levels of axon regeneration ~10-fold compared to PTEN deletion or treatment with Zymosan on its own (32).

1.5.3 TSC Deletion

TSC constitutes TSC1 and TSC2 that together form a complex to regulate cell growth (42). Akt phosphorylates TSC2, which stops the inhibitory effect of TSC on Rheb. Rheb can then activate mTOR (43). Research on over-expressing TSC in hippocampal neurons showed decreased axon growth (44). In comparison to that, knock-down of either TSC1 or TSC2 increased the number of neurons with several axons (44). Performing a conditional knockout of TSC1 in a mouse model resulted in high levels of p-S6 in injured RGC. The survival rate of RGC after injury was higher and axon regeneration was significantly enhanced in TSC-deleted mice compared to wild-type mice. However, the regenerative potential of RGC neurons in TSC-deleted mice was slightly lower than that in PTEN-deleted mice (41). This suggests that, despite mTOR signalling, other proteins regulated by PTEN also contribute to axon regeneration. Nevertheless, TSC deletion did enhance RGC survival after axotomy and induced axon regeneration.

1.5.4 Modulating RTP801 Expression

RTP801 supresses the activation of mTOR *via* release of TSC2 from the 14-3-3 protein (45). It is induced by a variety of factors, including DNA damage, oxidative stress, hypoxia and energy depletion (46-48) (Figure 2). Up-regulation of RTP801 in postmitotic neurons promoted apoptosis (49) Whereas, down-regulation of RTP801 seemed to have an anti-apoptotic effect on RGC in a mouse model of retinopathy (50). Also, research with neuroprogenitor cells shows that knockdown of RTP801 increased levels of p-S6 (51). Increased

levels of p-S6 indicated that inhibiting RTP801 might lead to increased cell growth and therefore axon regeneration. However, there has been no specific research carried out so far that shows that down-regulation of RTP801 in neurons also leads to axon regeneration.

1.5.5 Targeting RTP801 with siRNA in RGC

Using small interfering RNA (siRNA) as a method for RNA interference (RNAi) has become the method of choice to silence specific genes. It is performed in two main steps. The first step is the entrance of double stranded (ds) RNA into the cell where the enzyme Dicer chops it into smaller pieces, i.e. siRNA. siRNA is around 21-23 nucleotides long. The second step is the delivery of siRNA by Dicer to the RNA-induced silencing complex (RISC), which has RNase activity and uses the antisense siRNA strand to target mRNA to silence it (52). dsRNA has been successfully used in plants, worms and *Drosophila* to silence genes. However, in mammals dsRNA induced non-specific protein inhibition *via* an antiviral defence mechanism induced by interferon (IFN) (53). To prevent this, synthetic siRNA was developed that can avoid the initial antiviral-defence mechanisms while still being able to induce gene silencing (54).

Interfering with gene expression *via* RNAi is in a pre-clinical trial stage for neurodegenerative diseases at the moment and has shown some very promising results (55).

2. OBJECTIVES

The mTOR pathway is involved in regulation of cell growth and modulation of this pathway and has shown to enhance CNS axon regeneration. Data on a protein that seems to be an important regulator of the mTOR pathway, called RTP801, has not been published yet in association with CNS axon regeneration. In this study we want to investigate whether inhibiting RTP801 with siRNA, induces axon regeneration in rat RGC *in vitro* and *in vivo.* In addition, RGC will be treated with reagents that inhibit caspase-2 to prevent RGC apoptosis. We predict that inhibiting caspase-2 and RTP801 in RGC will increase RGC survival and enhance neurite growth *in vitro* and axon length *in* vivo.

3. MATERIALS AND METHODS

3.1 *In Vitro*

Unless otherwise stated reagents were obtained from Sigma-Aldrich (Poole, UK).

3.1.1 Retinal Dissection

To generate a culture of isolated retinal ganglion cells, eyes from Sprague Dawley (SD) rats (~200-250g) were used. Animals were sacrificed by rising concentrations of carbon dioxide (CO_2) in accordance with the UK Animals (Scientific Procedure) Act 1986.

The eyes were dissected out of the orbit with small dissection scissors and washed in cold sterile phosphate buffered saline (PBS, Gibco, Paisley, UK). Under a light microscope (Kyowa Tokyo) each eye was dissected individually under aseptic conditions. The eye was opened by puncturing the cornea with a scalpel and by cutting around the ora serrate with fine scissors. The cornea, lens and vitreous body was then removed with forceps to gain access to the retina. The retina was gently pulled apart from the loosely associated choroid with forceps and fully liberated by optic nerve excision (Figure 3).

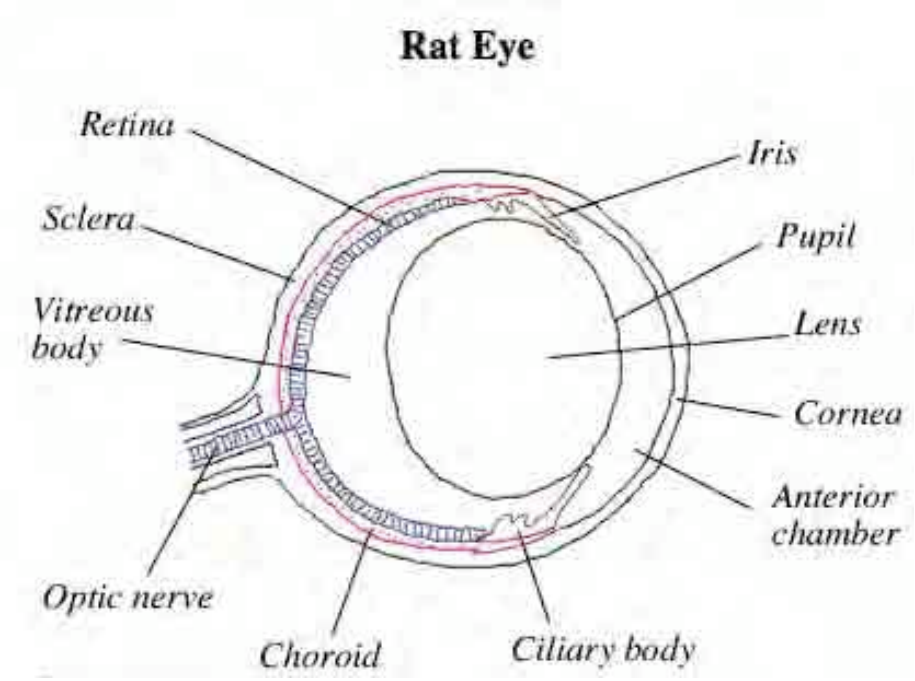

Fig 3. Anatomy of a rat's eye (Source of image: http://www.ratbehavior.org/Eyes.htm)

3.1.2 Retinal Culture

Four retinae were combined for each experiment and dissociated using a papain dissociation kit (Worthington Biochemicals, New Jersey, USA). Directly after removing the retinae from each eye, they were placed in a papain solution containing deoxyribonuclease I (DNase I) and chopped into small pieces with fine scissors. The solution was then incubated at 37°C in a humidified environment containing 5% CO_2 for 90 minutes. The cap of the tube was loosened to allow circulation of air. After the given time the tissue was triturated by pipetting up and down to generate a suspension of dissociated cells. The suspension was then placed into a 15ml Falcon tube and centrifuged at 300g for 5 minutes at 21°C. The supernatant was removed and the cells re-suspended in a solution containing 1.35ml Earle's Balanced Salt Solution (EBSS), 150µl of

reconstituted albumin ovomucoid inhibitor (AOI) and 75µl DNase I. The cell suspension was layered on top of 2.5ml AOI to create a discontinuous density gradient and centrifuged at 70g for 6 minutes at 21°C. After removal of the supernatant the cells were re-suspended in Neurobasal-A (NBA) supplemented with B27 supplement, L-Glutamine (200mM) and Gentimicin. A haemocytometer was used to calculate the number of live cells; these cells were subsequently plated at a density of 250 x 10^3 cells per well in laminin (20µg/ml) coated chamber slides (BD Biosciences, Oxford, UK). Cells were incubated for 1 day before administering the relevant treatment (Table 1).

3.1.3. Transfection of Retinal Culture

	Treatment groups	**Concentration**	**Company**
1	Lipofectamine	5µl/ml	Invitrogen
2	siRTP801*	20nM	QBI Enterprises
3	siRTP801* CNTF	20nM 10ng/ml	QBI Enterprises PeproTech
4	siRTP801* CNTF Z-VDVAD-FMK (caspase-2 inhibitor)	20nM 10ng/ml 100nM	QBI Enterprises PeproTech R&D Systems
5	CNTF	10ng/ml	PeproTech
6	Untreated control	n/a	n/a

Table 1. Types of treatment for retinal culture. * Length and sequence of siRTP801 is not available as it is currently involved in clinical trials

Retinal cultures were treated 1 day after set up. Three wells were used for one treatment group per culture. Lipofectamine 2000 (Invitrogen, Paisley, UK) was used to transfect RGCs with siRTP801 (QBI Enterprises, Ltd, Ness Ziona, Israel).

For treatment groups 2, 3 and 4, equal volumes of siRTP801 (1µl) and Lipofectamine (1µl) were added to 99µl of Opti-MEM and incubated separately for 20 minutes at room temperature. At the end of the designated time, both solutions were mixed together and left for another 20 minutes at 37°C. For treatment group 1, 1µl Lipofectamine and 199µl Opti-MEM were incubated for 20 minutes at 37°C. After supplemented NBA had been removed from the cell culture, 200µl of either the siRTP801-liposome or Lipofectamine mixture were added to a well. Treatment groups 5 and 6 were treated with 200µl Opti-MEM (Table 1). Cultures were then incubated at 37°C in a humidified environment containing 5% CO_2 for 5 hours.

After 5 hours had elapsed, the transfection solution was removed and either 500µl of supplemented NBA for treatment group 1, 2 and 6, supplemented NBA and CNTF (PeproTech, London, UK) for treatment group 3 and 5, or supplemented NBA, CNTF and Caspase (Casp)-2 inhibitor (R&D Systems, Oxfordshire, UK) for treatment group 4 was added pre-warmed to 37°C per well (Table 1). The cultures were then incubated for further 2 days prior to analysis.

3.1.4 Immunocytochemistry

After 2 days of treatment the medium of the cell culture was aspirated and cells were fixed for 10 minutes in 4% paraformaldehyde (PFA; TAAB Laboratories Berkshire, UK) in Tris Buffered Saline (TBS; pH 7.3). After three washes in a beaker with TBS for 10 minutes, the cells were blocked with blocking buffer (Table 2) for 20 minutes. Each well was then treated with 150µl of a monoclonal mouse antibody against βIII-tubulin and monoclonal rabbit antibody against phosphorylated (phospho) mTOR (Cell Signalling, Herts, UK) or polyclonal rabbit antibody against phospho-mTOR (Abcam, Cambridge, UK) at a 1:200 dilution for 1 hour. All antibodies were diluted in antibody dilution buffer (Table 2). After 1 hour, chamber slides were washed 3 times in a beaker with TBS for 10 minutes. Secondary antibodies, Alexa Fluor 488 goat anti-rabbit IgG and Texas red goat anti-mouse IgG (both Molecular Probes, Invitrogen, Paisley, UK), were then applied in a 1:400 dilution and incubated for 1 hour covered by aluminium foil to prevent bleaching of fluorescence. Chamber slides were washed 3 times in a dark beaker containing TBS for 10 minutes. The chamber was then removed and slides were mounted in Vectashield with DAPI (Vector Laboratories, Peterborough, UK). Slides were viewed with an epi-fluorescent microscope and Axiovision software was used to capture images (both Carl Zeiss MicroImaging, LLC, Thornwood, NY).

Solutions	Reagents
Tris Buffered Saline (TBS)	50mM Tris-HCl, 150mM NaCl, Trizma base in milli-Q water
Blocking Buffer	3%Bovine serum albumin (BSA), 1% TritonX inTBS
Antibody Dilution Buffer	3%BSA, 0.5% Tween20 in TBS

Table 2. Solutions for immunocytochemistry

3.1.5 Statistical Analysis

Each experiment was performed at least in duplicate on separate occasions. For cell analysis three wells containing the same treatment were each separated into 9 equally sized squares. One image was randomly taken per square using an epi-fluorescent microscope and Zeiss camera and analysed using Axiovision software (Carl Zeiss MicroImaging, LLC, Thornwood, NY). Data from the images was averaged and plotted as graphs. No statistical analysis was carried out as only two independent experiments were performed.

3.2 *In Vivo*

3.2.1 Surgical Procedure

The study used three adult Sprague Dawley rats (~150-250g) in each experimental and control group. All procedures were carried out in accordance with regulations of the UK Animals (Scientific Procedures) Act 1986 under a home office license. Optic nerve crush (ONC) surgeries were performed by Professor Martin Berry, intravitreal (ivit) injections were performed by Jenna

O'Neill and anaesthesia/analgesia were administered by various members of the Molecular Neuroscience Group. All procedures were observed by myself.

The animals were initially anaesthetised with 4% isoflurane (Abbott Laboratories Ltd, Kent, UK); the dose was then reduced to 3% and maintained at this level throughout the procedure. Animals received a subdermal injection of the analgesic Buprenorphine (National Veterinary Supplies, Stoke-on-Trent, UK) at a dose of 0.03mg/kg prior to surgery. A lubricant was also applied to the cornea to prevent dehydration (Lacri-Lube, Allegan, High Wycombe, UK).

3.2.2 Optic Nerve Crush

The experimental and control group both underwent bilateral ONC at the start of the study. After the rat had been anaesthetised, the head was shaved and the rat placed into a David Kopf stereotaxic instrument. A central rostro-caudal incision was made in the skin on top of the skull. To expose the orbital margin, the skin was slightly pulled over the upper lid and the fascia was mobilised. A vertical incision was made into the temporalis muscle and the incision was continued rostrally of the orbital margin. Care was taken to ensure that the supraorbital vessels did not get injured. Prior to cutting through the supraorbital nerve, the vessels around the nerve were crushed to avoid bleeding. The Harderian gland was exposed by removing its capsule and moved rostrally to access the ON. To expose the ON, retractors were inserted between the ON and Harderian gland and between the medial rectus muscle and ON. The retractor bulbi muscle and the dural sheath around the ON was then cut to access the ON. Care was taken to maintain the integrity of the central retinal artery that runs through the dural sheath. The ON was then crushed 2mm distal

from the eyeball (Figure 4). After the crush the retractors were removed and the rectus muscles, Harderian gland and skin were placed back to their original position. The same procedure was then carried out on the second ON. After two successful ONCs the skin margins were sutured.

3.2.3 Lens Injury

Immediately after the ONC, the experimental and control groups received bilateral lens injury. The tip of a 19 gauge needle was inserted through the sclera immediately posterior to the ora serrate and perpendicular to the axis of the ON. The needle tip was then moved across the surface of the lens to induce injury to the lens capsule.

3.2.4 Intravitreal Injections

A glass micropipette was loaded with 10µl of the relevant treatment (Table 3) and attached to a syringe. The micropipette was then inserted into the vitreous body through the sclera immediately posterior to the ora serrate (Figure 4). The solution was injected slowly into the vitreous body to ensure adequate diffusion. Both eyes of each animal in the experimental (n=3) and control group (n=3) received injections stated below (Table 3). After the first injection, injections were carried out every 8 days over the experimental period (three times in total). Animals were sacrificed by rising concentrations of CO_2 after 24 days.

	Treatment	Volume	Concentration
Experimental Group	siRTP801* siCasp-2*	5µl 5µl	20µg/ml 20µg/ml
Control Group	siEGFP*	10µl	20µg/ml
* QBI Enterprises, Ltd, Ness Ziona, Israel			

Table 3. Treatment groups for *in vivo* experiment

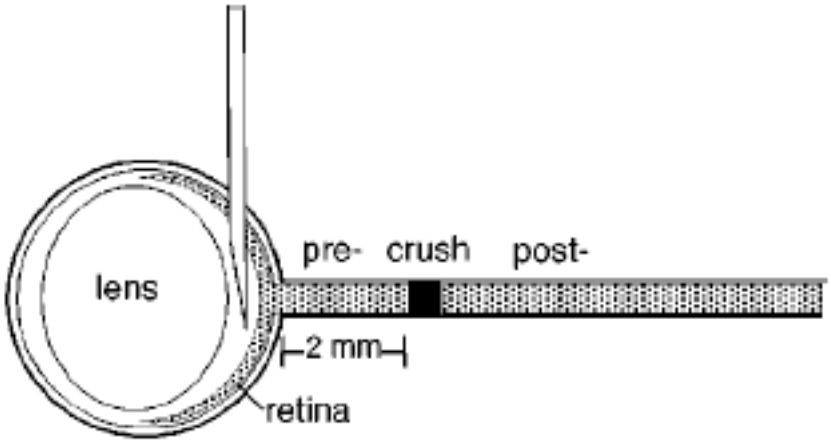

Fig 4. ON was crushed 2mm distal from the eyeball. Lens injury was induced just after ONC. Ivit injections were performed every 8 days. Solutions for both groups were injected into the vitreous body. (Source of image: Leon et al., 2000)

3.2.5 Tissue Preparation for Histology

On day 24 post-ONC, animals were given a lethal overdose of CO_2 and perfused intracardially with 300ml PBS followed by 300ml 4%PFA in PBS. The ON segments, with the chiasm still attached, were dissected free from connective tissue and post-fixed in 4%PFA at 4°C overnight. The ON were then

placed sequentially through sucrose gradients to cryoprotect the tissue. This involved placing the tissue in 30%, 20% and 10% sucrose solutions in PBS at 4°C overnight. The nerves were then embedded in OCT embedding medium (R.A. Lamb Laboratory, Cheshire, UK). ON sections of 15µm were cut longitudinally on a cryostat (Bright Instrument Company, Huntingdon, UK). The sections were thaw-mounted onto coated glass slides (Leica Microsystems, Peterborough, UK) and dehumidified at 37°C overnight to increase adhesion. Slides were kept at -80ºC for long-term storage.

3.2.6 Immunohistochemistry

Due to limited time one ON instead of both ON per animal were stained and analysed. The sections were defrosted at room temperature and washed in rinsing buffer (Table 4) three times for 5 minutes. Rinsing buffer around the ON was aspirated and a hydrophobic pen was used to draw a circle around each section. Sections were then incubated with 200µl blocking buffer (Table 4) in a humidified chamber for 1 hour at room temperature. After the time had elapsed, sections were treated with 200µl of a monoclonal mouse antibody against neuronal growth-associated protein GAP-43 (Invitrogen, Paisley, UK) and polyclonal rabbit antibody against Laminin (Sigma-Aldrich) at a 1:500 dilution at 4°C in a humidified chamber overnight. Sections were washed in rinsing buffer three times for 5 minutes. Secondary antibodies Alexa Fluor 488 goat anti-mouse IgG and Alexa Fluor 594 goat anti-rabbit IgG (both Molecular Probes, Invitrogen, Paisley, UK) were then applied in a 1:500 dilution and incubated at room temperature for 1 hour in a dark humidified chamber to prevent bleaching of fluorescence. Sections were washed in rinsing buffer three times for 5

minutes and then mounted in Vectashield with DAPI (Vector Laboratories, Peterborough, UK). They were viewed with an epi-fluorescent microscope and the Axiovision software was used to capture images (both Carl Zeiss MicroImaging, LLC, Thornwood, NY).

Solutions	Reagents
10mM PBS	PBS tablets in milli-Q water
Rinsing Buffer	0.1% TritonX in PBS
Blocking Buffer	10% New-born goat serum, 3% BSA in rinsing buffer
Antibody Dilution Buffer	3% BSA in rinsing buffer

Table 4. Solutions for immunohistochemistry

3.2.7 Statistical Analysis

Axon growth was quantified by counting the number of GAP-43 positive axons within 200-500μm, 500-1000μm, 1000-1500μm and 1500-2000μm distal to the crush site.

An N value of 3 was obtained. The Student T Test was carried out and a P value of < 0.05 was considered as significant.

4. RESULTS

4.1 *In Vitro* Studies

4.1.1. Identification of mTOR Activation in RGC

To investigate whether inhibiting RTP801 activates the mTOR pathway and therefore leads to RGC axon regeneration, primary retinal cultures containing RGC were treated with siRTP801 to knock down gene expression. Due to a limited amount of time the *in vitro* experiments could only be carried out in duplicate. RGC were characterised by being immunopositive for βIII-tubulin, spherical, having no more than two neurites and large nuclei counterstained with DAPI. To demonstrate mTOR activation RGC were stained with an antibody against phospho-mTOR. For most of the experiments phospho-mTOR from Cell Signalling was used. This antibody stained βIII-tubulin positive RGC extremely weakly producing a signal no greater than the no primary control (Figure 5). As such, the generated images were deemed to be immunonegative and this antibody was not used in future experiments. The phospho-mTOR antibody from Abcam was used as an alternative and generated stronger βIII-tubulin positive RGC immunostaining (Figure 5). However, both antibodies stained all βIII-tubulin positive RGC irrespective of treatment so that a differentiation between an untreated control and siRTP801 treated RGC was not possible. Therefore, both antibodies were not used to demonstrate activation of mTOR. Instead the functional outcome (i.e. RGC survival and neurite outgrowth) was used to determine if the mTOR pathway had been activated by siRTP801 treatment.

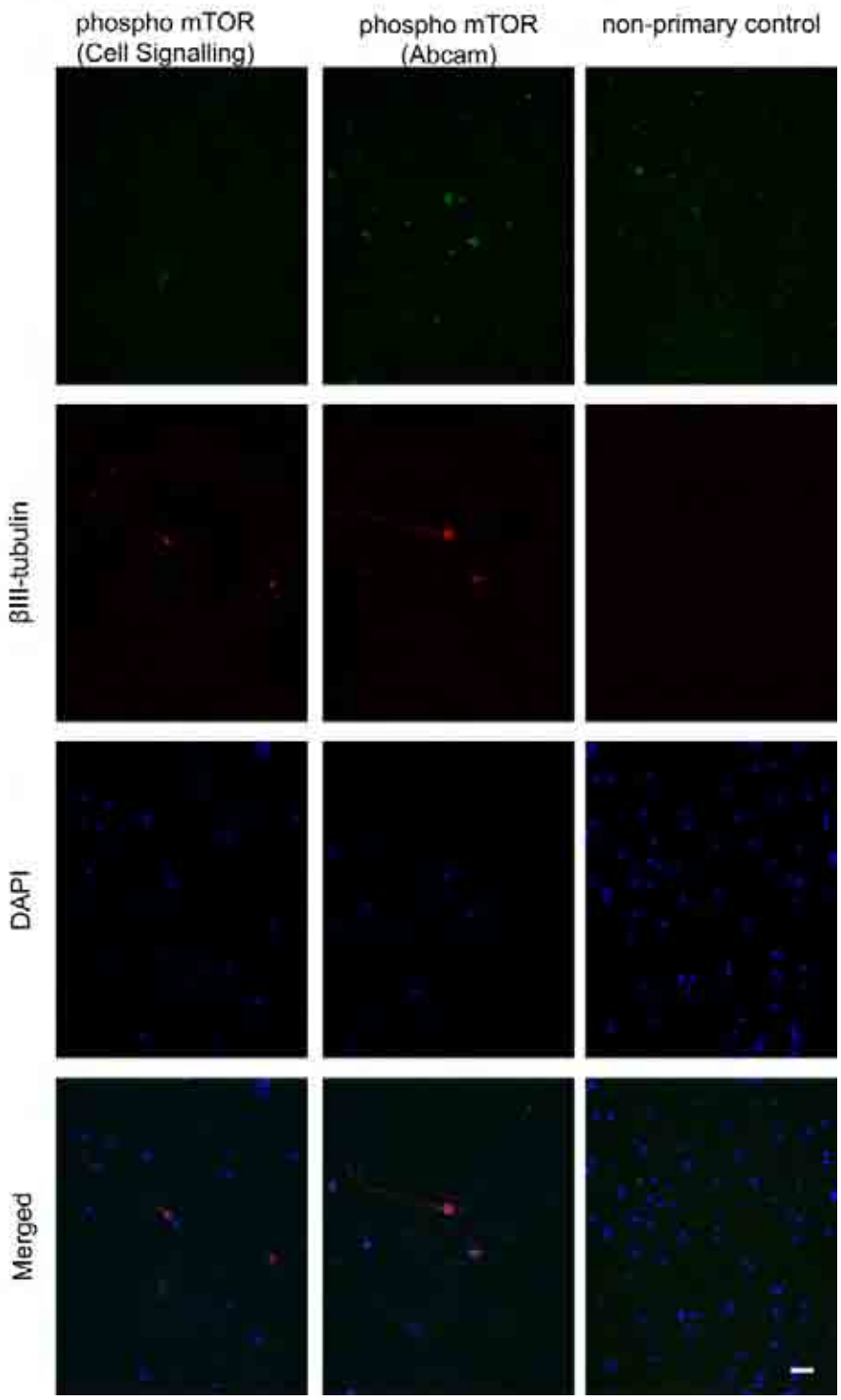

Fig 5. βIII-tubulin positive RGC were immunostained with two different antibodies against phospho-mTOR. Phospho-mTOR from Cell Signalling produced an extremely weak signal. Phospho-mTOR from Abcam produced a stronger signal that correlated with the βIII-tubulin positive RGC. The no primary control was used as a comparison and to asses antibody specificity. Scale bar, 50μm

4.1.2 The Effect of siRTP801, CNTF and Caspase-2 Inhibitor on RGC Survival

Since there is no data regarding the effect of inhibiting RTP801 on RGC survival, primary retinal cultures were treated with siRTP801 alone or in combination with CNTF or CNTF and Casp-2 inhibitor. As the experiments were only carried out in duplicate no statistical analysis was performed.

The number of surviving βIII-tubulin positive RGC in the treatment groups (Table 1; Lipofectamine, CNTF, siRTP801, siRTP801+CNTF and siRTP801+CNTF+Casp-2 inhibitor) was compared to an untreated control. All treatment groups tended to have high survival rates (Figure 6). Treatment with Lipofectamine, CNTF and siRTP801+CNTF enhanced survival (≥100%). Lipofectamine and CNTF treated RGC had the highest survival rates (≥125%). siRTP801 alone did not increase cell survival. Treatment with siRTP801, CNTF and Casp-2 inhibitor slightly reduced survival (90%), which was unexpected as caspase-2 is a pro-apoptotic enzyme (Figure 6).

Overall, the treatment groups that were treated amongst other reagents with siRTP801 had lower survival rates compared to CNTF treated groups and only the siRTP801+CNTF group had higher survival rates compared to the control. It appears to be a trend that inhibiting RTP801 does not enhance survival. However, the small replicate number of each treatment group prevented the significance of the difference being assessed.

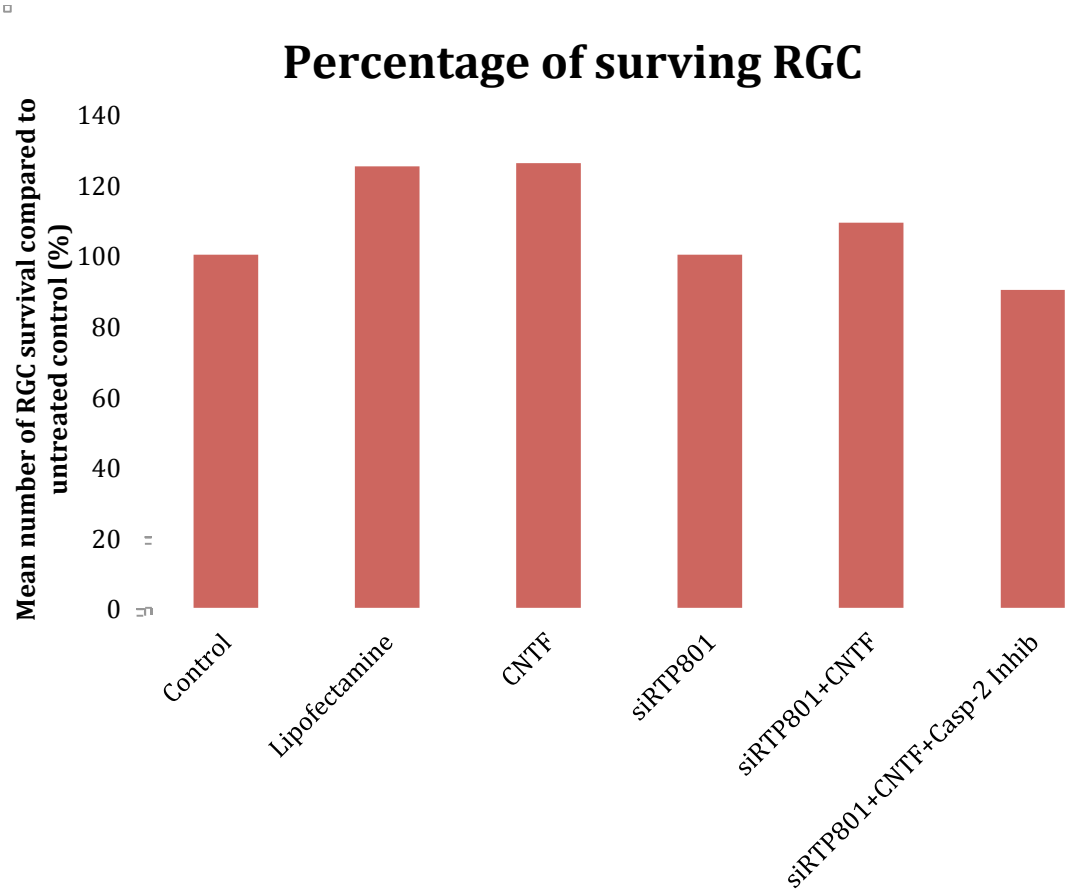

Fig 6. Mean percentage of surviving primary RGC in response to treatment with siRTP801, CNTF and Casp-2 inhibitor. Each experiment was performed in duplicate on separate occasions except treatment with Lipofectamine, which was performed three times.

4.1.3.Number of RGC with Neurites

Modulating the mTOR pathway in RGC *in vivo* by inhibiting PTEN or TSC significantly enhanced neurite outgrowth (41). However, the effect of modulating the mTOR pathway in RGC *in vitro* has never been reported.

A neurite was defined as any RGC projection longer than one cell soma in diameter. The Lipofectamine group exhibited a slightly higher number of RGC with neurites compared to the untreated control. CNTF treatment enhanced neurite outgrowth the most out of all treatment groups. Treatment with siRTP801

alone did not promote neurite outgrowth and may have even caused minor inhibition. When siRTP801 was added in combination with CNTF, the number of RGC with neurites was greater than control but less than that of CNTF alone. The siRTP801-CNTF-Casp-2 inhibitor group induced the same level of neurite outgrowth (Figure 7) but caused reduced RGC survival than siRTP801 and CNTF treatment (Figure 6). Altogether treating RGC with siRTP801 on its own enhanced neurite outgrowth the least compared to all other treatment groups whereas treatment of siRTP801 in combination with CNTF or CNTF and Casp-2 inhibitor enhanced neurite outgrowth.

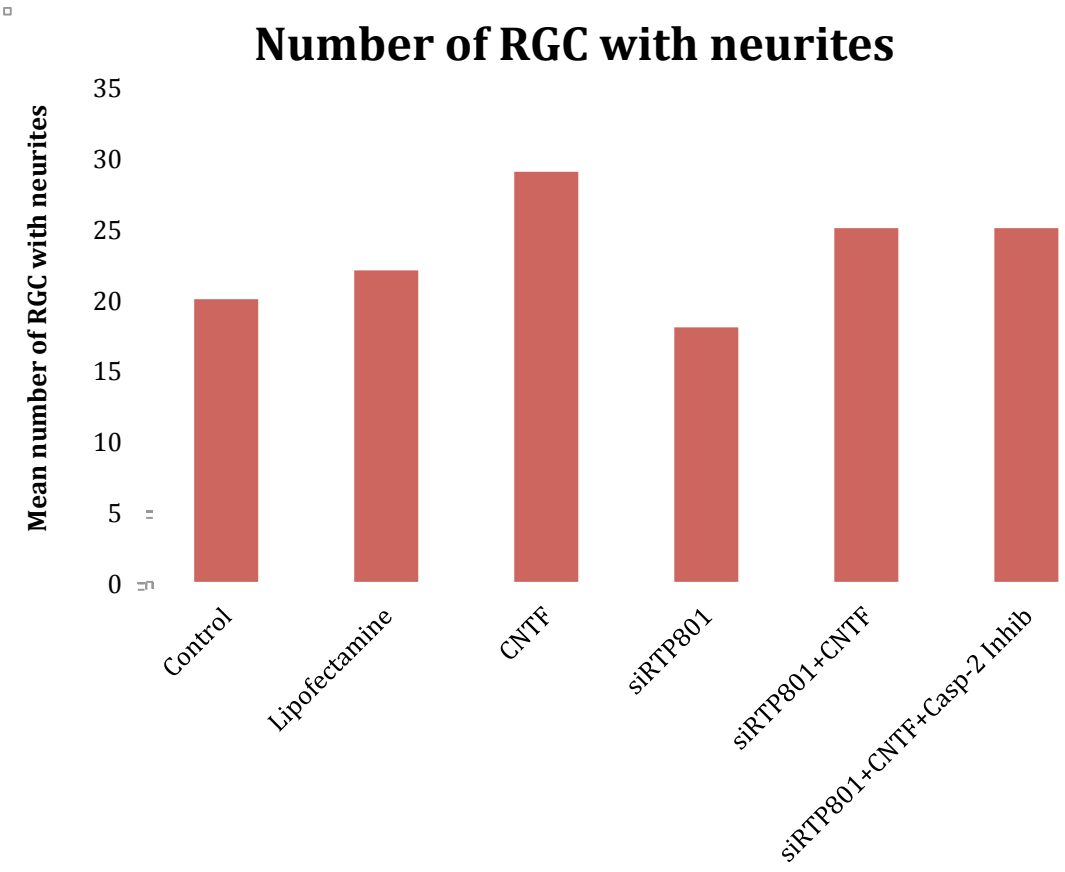

Fig 7. Mean number of RGC with neurites in response to treatment with siRTP801, CNTF and Casp-2 inhibitor. Each experiment was performed in duplicate on separate occasions except treatment with Lipofectamine, which was performed three times.

4.1.4 Stimulation of RGC to Increase Neurite Length

Neurite length was measured using Image Pro Software to investigate whether activation of mTOR *via* siRTP801 increased neurite length. The untreated control group and the Lipofectamine group both induced similar low levels of neurite outgrowth (Figure 8). This indicates that the Lipofectamine reagent did not have an adverse effect on neurite outgrowth and survival. CNTF treatment appeared to enhance RGC survival and neurite outgrowth (Figure 6,7,and 8). siRTP801+CNTF enhanced neurite length more than siRTP801 and CNTF alone. In fact treatment with siRTP801+CNTF increased neurite length ~ 2-fold compared to untreated and Lipofectamine controls. The combination of siRTP801, CNTF and Casp-2 inhibitor had the greatest impact on neurite length inducing a ~ 3-fold increase compared to untreated and Lipofectamine controls and a ~ 2-fold increase compared to CNTF and siRTP801 group (Figure 8). Figure 9 illustrates examples of neurite length of βIII-tubulin positive RGC stimulated by each treatment group. RGC are stained with βIII-tubulin and nuclei are stained with DAPI. As can be observed from Figure 6, the longest neurites were detected in RGC cultures treated with siRTP801+CNTF+Casp-2 inhibitor compared to untreated control and Lipofectamine groups, which contained βIII-tubulin positive RGC without neurites.

Although treatment with siRTP801+CNTF+Casp-2 inhibitor hardly enhanced βIII-tubulin positive RGC survival and outgrowth, it did however, enhance neurite length strongly compared to the other treatment groups *in vitro*. Therefore, the combination of caspase-2 and RTP801 inhibition was also tested *in vivo* to evaluate effects on RGC axon regeneration.

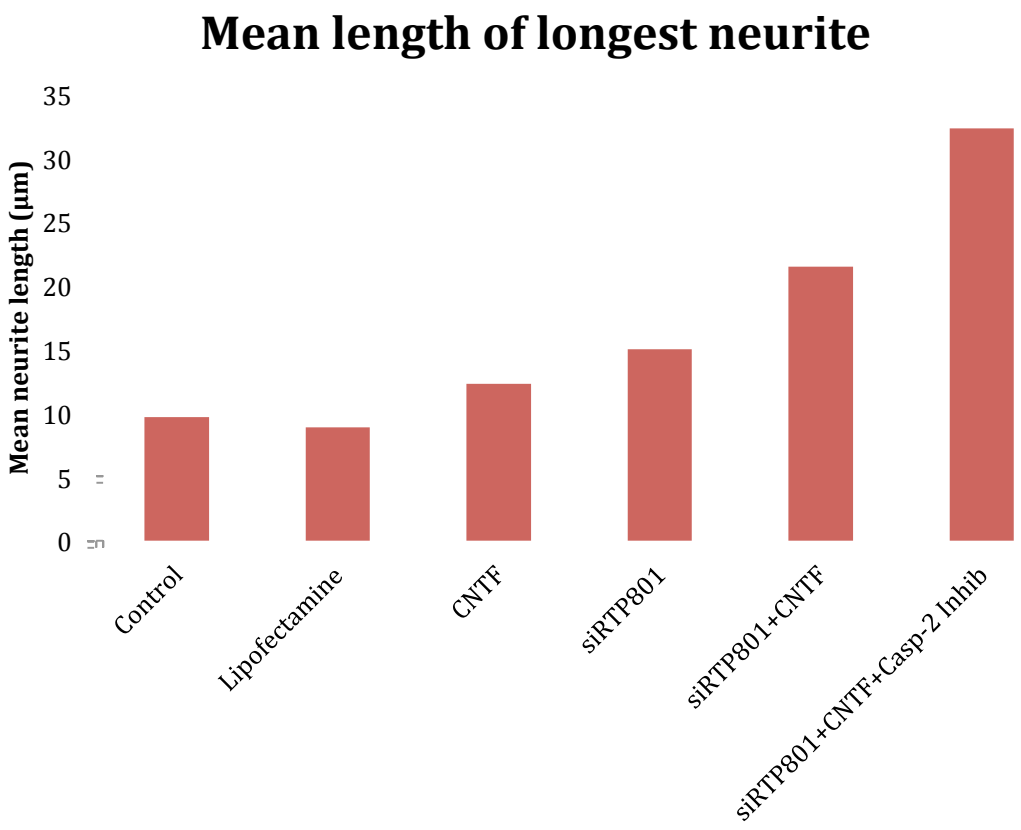

Fig 8. Mean length of longest neurite per βIII-tubulin positive RGC in response to treatment with siRTP801, CNTF and Casp-2 inhibitor. Each experiment was performed in duplicate on separate occasions except treatment with Lipofectamine, which was performed three times.

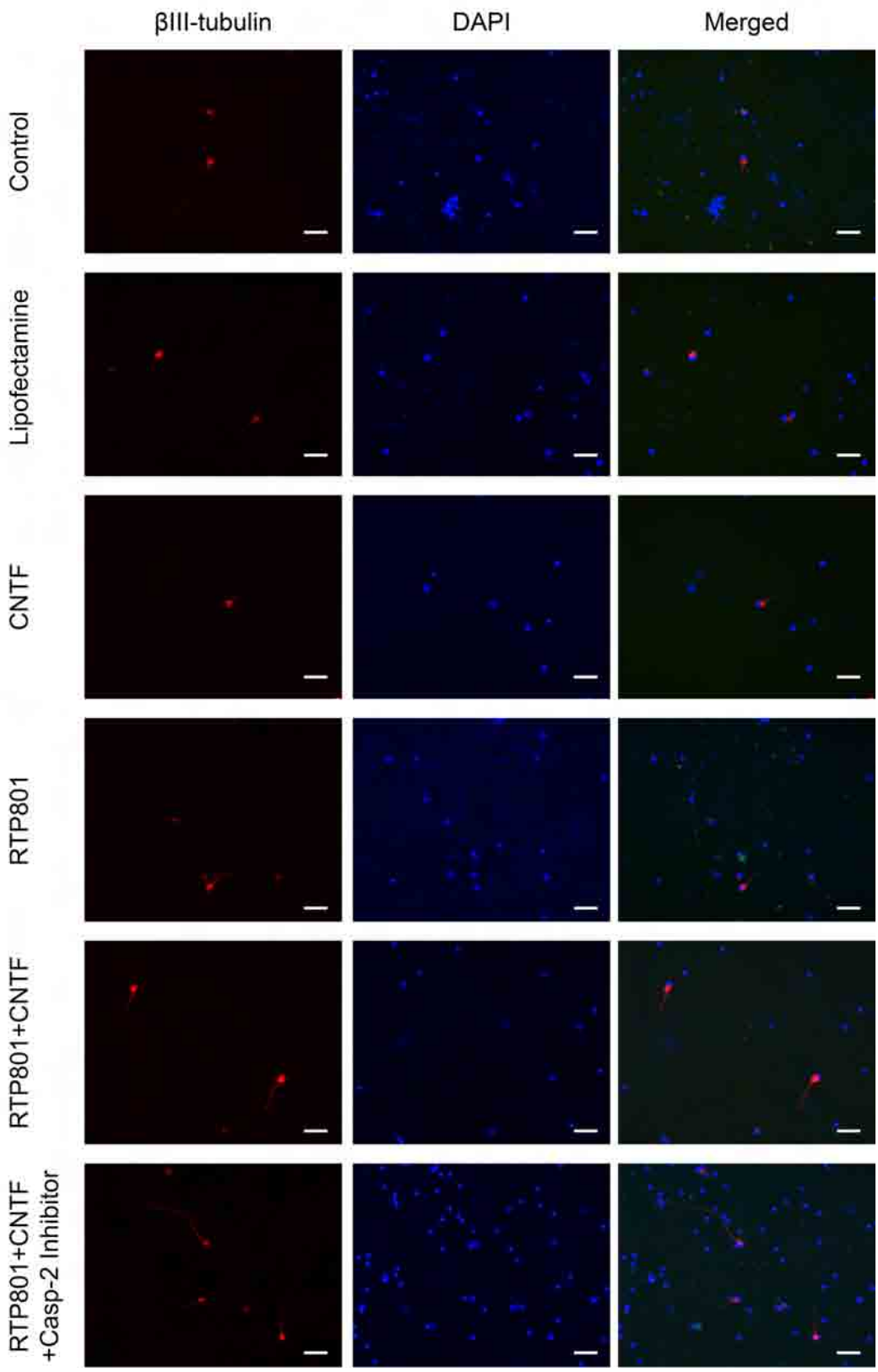

Fig 9. Examples of βIII-tubulin positive RGC counterstained with DAPI that have been treated with various treatments. Scale bar, 50μm.

4.2 *In Vivo* Studies

To investigate the effect of stimulating mTOR signalling by inhibiting RTP801 and prolonging RGC survival using siCasp-2 (4) on axon growth *in vivo,* siRTP801 and siCasp-2 were injected into the vitreous body of adult rats every 8 days for 24 days after they received ONC with a lens injury to induce RGC axon outgrowth (27,29). Control animals received ONC and lens injury but were injected with a non-targeting siRNA (siEGFP).

To determine whether siCasp-2 prevented apoptosis in RGC, GAP-43 positive axons in the proximal segment of the ON, before the site of ONC, were counted in the experimental and control groups. Axons were counted along a vertical line drawn across the ON (200µm before the site of ONC). To analyse whether blocking RTP801 and activating the mTOR pathway enhanced axon elongation through the lesion site, GAP-43 positive axons were counted in the distal ON post-ONC. Axons were counted in an area 200-500µm, 500-1000µm, 1000-1500µm and 1500-2000µm distal to the site of ONC.

As it was not possible to specify continuous axons, as they go in and out of the plane of view, each GAP-43 positive axon segment (Figure 10; see white arrows) was counted and defined as one axon.

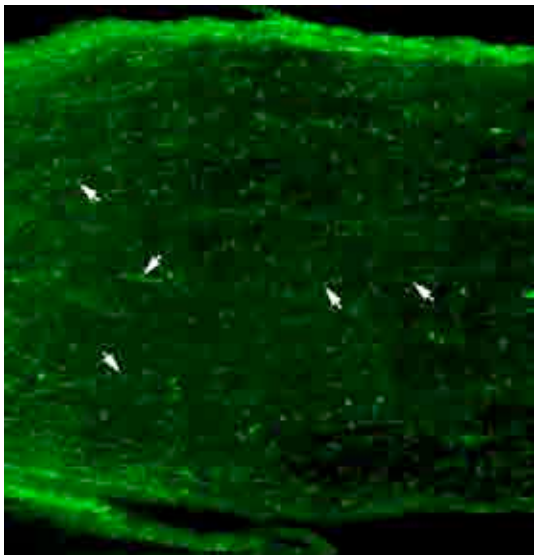

Fig 10. Part of an ON distal to the site of ONC. Each GAP-43 positive axon (indicated by a white error) was counted to determine the regenerative potential of modulating the mTOR pathway *via* siRTP801

4.2.1 Optic Nerve Regeneration In Vivo

At 24 days after the ONC, levels of axon regeneration were determined by GAP-43 immunohistochemistry. Treatment with siRTP801 and siCasp-2 enhanced lens injury-induced survival of RGC axons proximal to the site of ONC as expected (Figure 11.A.I and 12). Treatment with siEGFP also appeared to enhance RGC survival (Figure 11.B.I and 12). It was less compared to the experimental group but no significant difference between both groups was detected (p >0.05). Furthermore, both groups showed a similar amount of axon regeneration distal to the site of ONC (Figure 11). Higher numbers of GAP-43 positive axons were detected in the centre of the ON of the experimental group (Figure 11.A.II). In the control group more axons were present at the margins of the ON than the centre at the same distance distal to the ONC (Figure 11.B.III). Axons that were growing along the edges of the ON grew a relatively long distance in both groups (Figure 11.A.IV and 11.B.IV). Few axons in the centre of

the ON grew longer distances than axons present at the margins (Figure 11.A.V and 11.B.V).

Overall, treatment with siRTP801 and siCasp-2 slightly enhanced lens injury-induced survival of RGC axons but with no significant difference to treatment with siEGFP. Furthermore, no significant difference between both treatment groups was detected distal to the site of ONC ($p > 0.05$) (Figure 13).

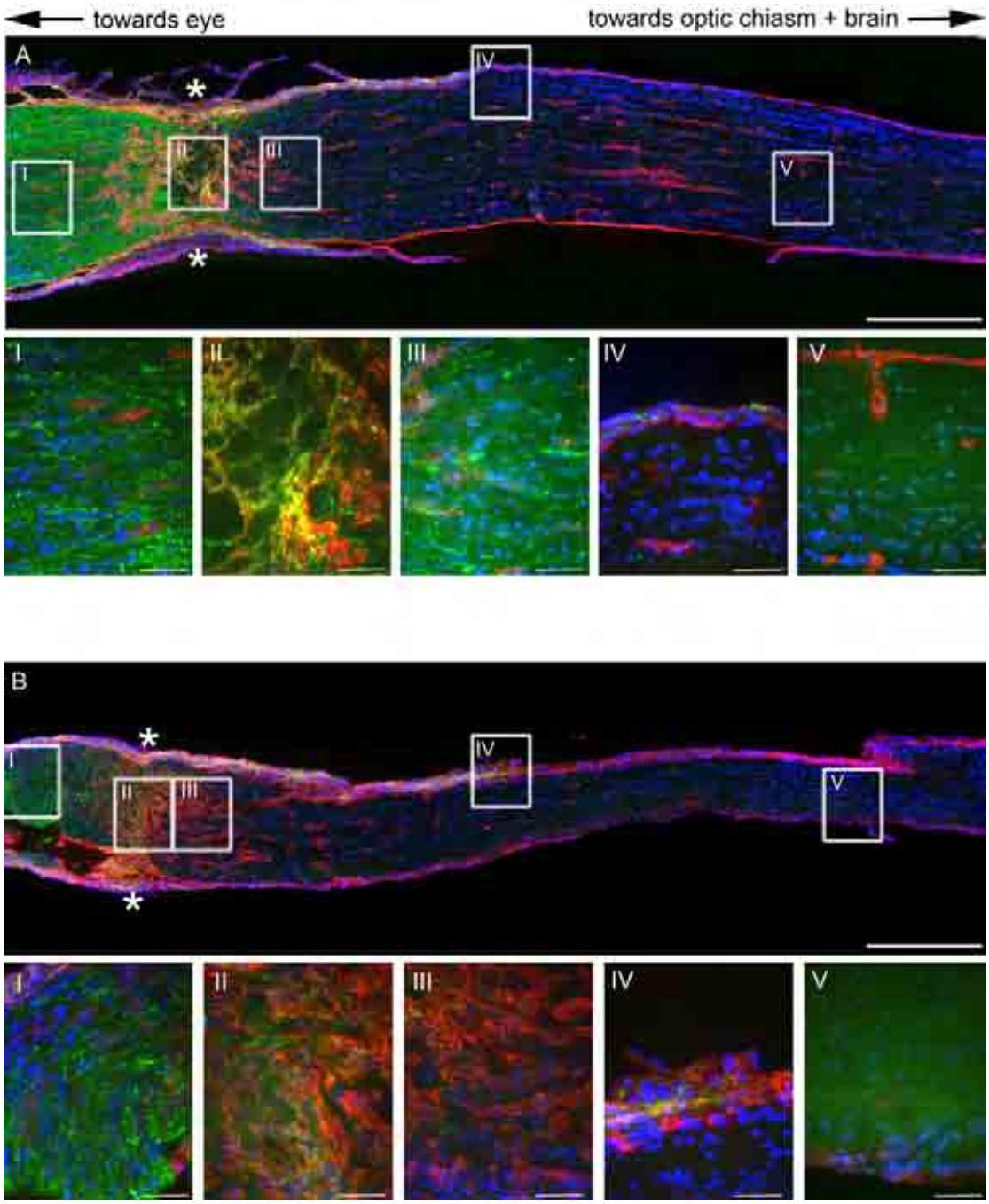

Fig 11. Longitudinal sections of ON immunostained to detect GAP-43 positive axons proximal and distal to the injury site (asterisk) 24 days after ONC. Rats were injected with siRTP801 and siCasp-2 (A) or with siEGFP (B) after lens injury and ONC, Scale bar, 200µm. X40 magnifications of nerves (A I-IV) and (B I-IV) Scale bar for inserts, 30µm.

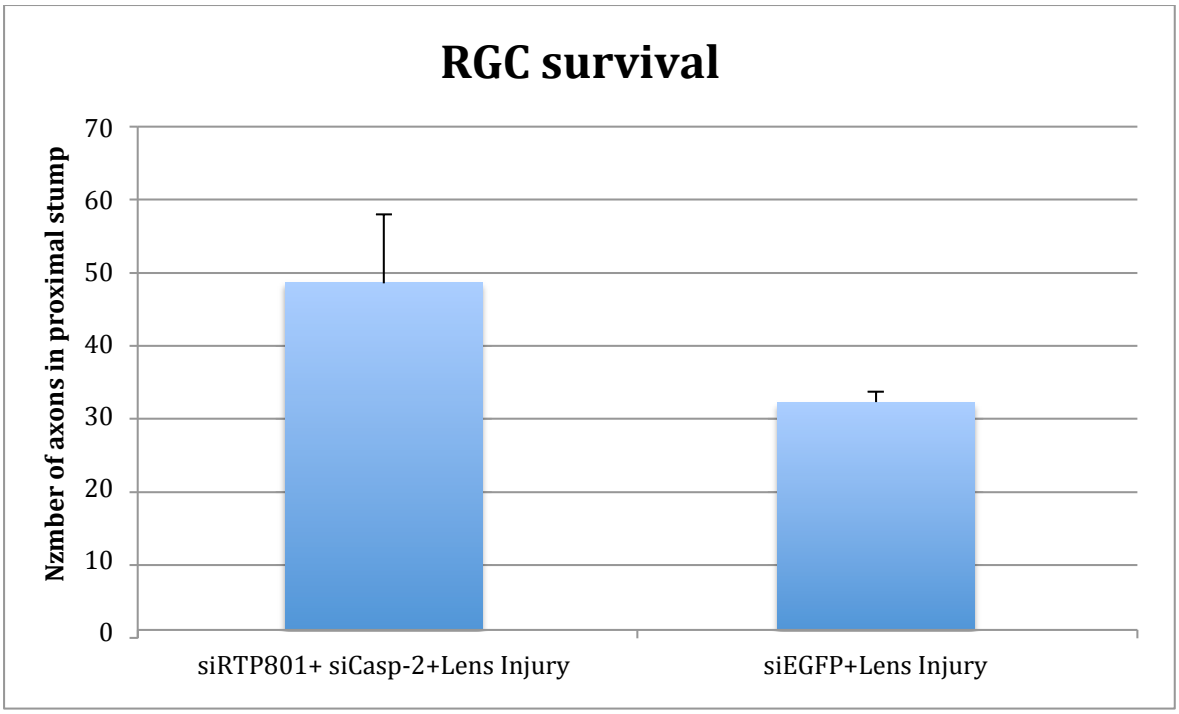

Fig 12. Quantification of RGC survival by counting GAP-43 positive axons 200µm proximal to the site of the ONC. Values are means ± SEM. n=3

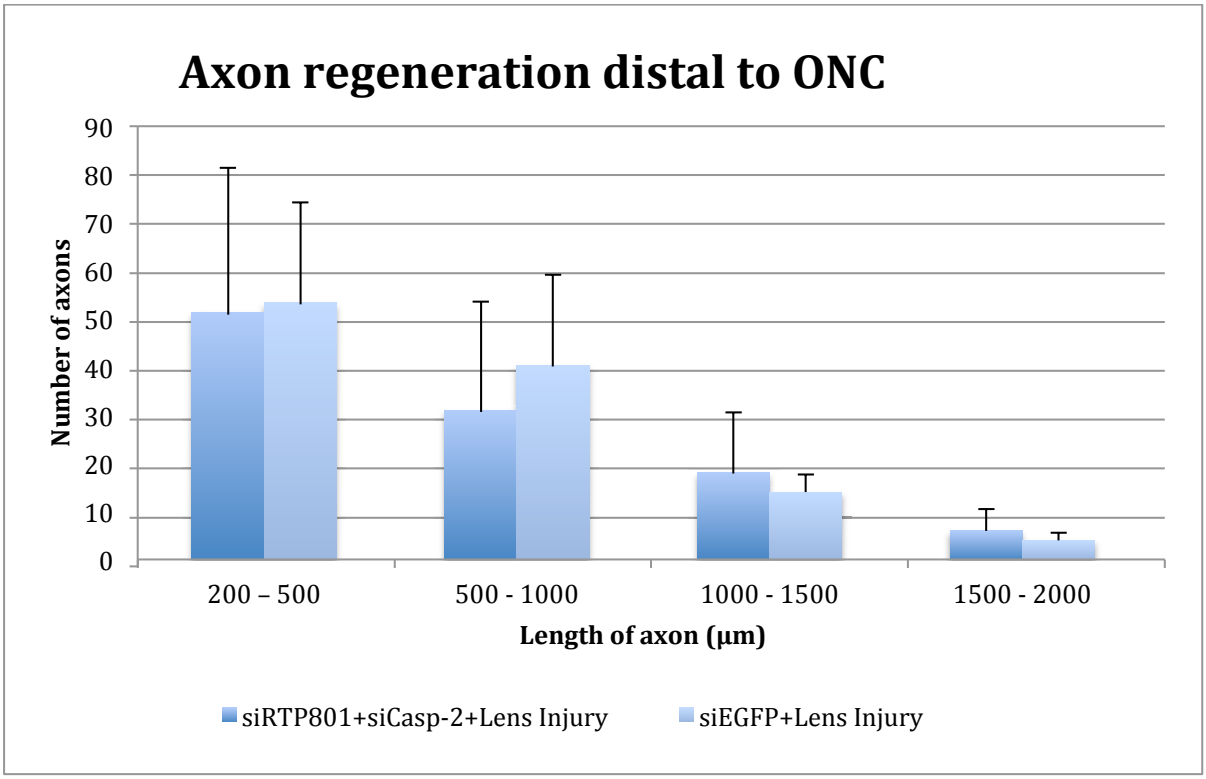

Fig 13. Quantitation of axon regeneration by counting GAP-43 positive axons distal to the site of the ONC. Values are means ± SEM. n=3

4.2.2 Response of Individual Animals to siRTP801 and siCasp-2

Since animals responded to the treatment in different ways, we analysed the data from individual animals to understand our findings from this study better. Animal 1 in the experimental group responded very well to the treatment with over 40 axons reaching 1000µm and 15 axons reaching 1500µm and beyond. Animal 2 and 3 on the other hand showed a weak or minimal response to the treatment with siRTP801 and siCasp-2 (Figure 14A). A similar variability amongst individual animals was also observed in the control group. In this group, animal 1 showed a stronger reaction to the treatment than animal 2 and 3 but the variation between the animals that responded to those that did not is less compared to the experimental group (Figure 14B).

The number of GAP-43 positive axons from the responding animal (Animal 1, Figure 14A) in the experimental group was ~ 2-fold higher at 1000-1500µm and 1500-2000µm compared to the responding animal (Animal 1, Figure 14B) from the control group. Although the average number of GAP-43 positive axons from all animals of each group does not show great difference, the difference between axon regeneration from the responding animals of each group is much greater.

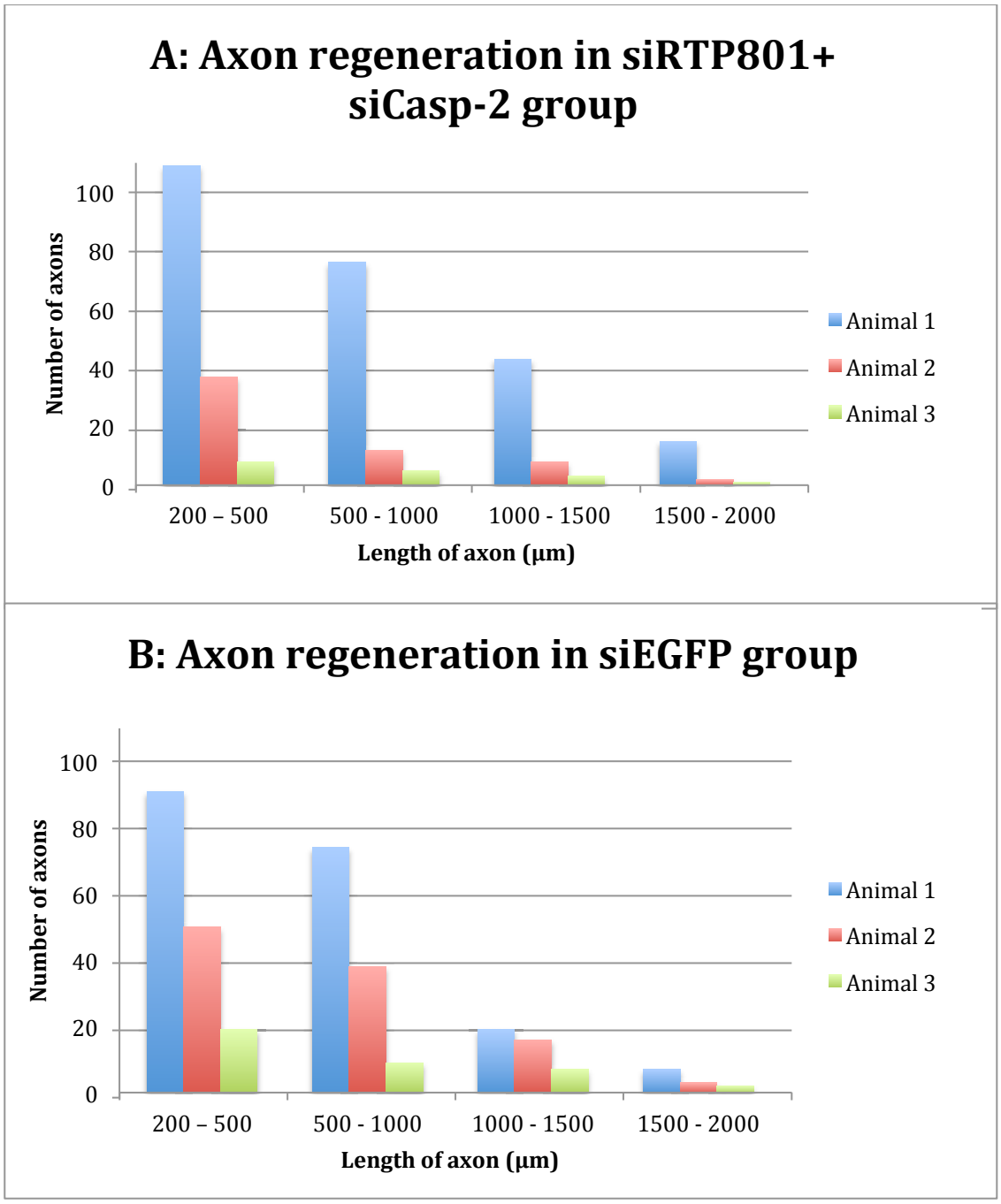

Fig 14. Quantitation of axon regeneration in individual animals by counting GAP-43 positive axons distal to the site of the ONC. Every eight days animals received injections with siRTP801 and siCasp-2 (A) and siEGFP (B).

5. DISCUSSION

After injury to the CNS, axon regeneration is crucial to prevent irreversible neurological deficits. The pathophysiological process of CNS injury is still very limited and hence prevents the discovery of novel treatments for people with CNS injury. Several animal studies have shown that axon regeneration is possible (26,27,29,32). However, for treatment in humans it is necessary that the reagents used for axon regeneration are safe and affordable.

Treatment for various diseases with siRNA has gained more and more interest. A siRNA, against human RTP801 (PF-655) provided by the same company (Quark Pharmaceuticals) as the siRNA used for this study, is currently in a Phase II clinical trial for treatment of wet age-related macular regeneration (AMD) and diabetic macular oedema (DME) (http://www.quarkpharma.com/qbi-en/products/53/). As this siRNA shows promising results for AMD and DME the overall aim for this study was to investigate the effect of siRTP801 on axon regeneration *in vitro* and *in vivo*.

5.1 *In Vitro* Studies

5.1.1 Activation of the mTOR Pathway

Phospho-mTOR antibodies from two different companies were used to immunostain βIII-tubilin positive RGC to determine whether mTOR had been activated by inhibiting RTP801. The phospho-mTOR antibody from Cell Signalling immunostained βIII-tubilin positive RGC more weakly than the

phospho-mTOR antibody from Abcam and staining could not be distinguished from a no-primary control. Although the phospho-mTOR antibody from Abcam immunostained βIII-tubilin positive RGC strongly, there was no difference in staining intensity between untreated controls and siRTP801 treated RGC. To be able to determine whether mTOR has been activated a quantitative technique such as western blot or post-transcriptional regulation should be used.

The reason why the untreated controls were immunopositive for phospho-mTOR could be because of a stress response induced by tissue dissociation and cell culture. Therefore a positive and negative control needs to be used in future experiments to determine antibody specificity and levels of mTOR activation. Once this has been determined, each of the antibodies can be optimised and used or excluded from future experiments. In addition to this, mTOR activation could be confirmed using an antibody targeted against mTOR's substrate such as phospho-S6. Antibodies against phospho-S6 have been used in several studies as a reliable way to monitor activation of mTOR (41,51). As mTOR activation in RGC could not be determined by immunocytochemistry, we decided to focus on the functional outcomes associated with siRNA treatment.

5.1.2 Functional Effect of siRNA Treatment

In vitro, RGC were treated with different combinations of siRTP801, CNTF and Casp-2 inhibitor.

Choosing a siRNA (siRTP801) as a method to silence specific genes has become very popular in research and has shown promising results for therapeutic purposes. Treatment of RGC with siRTP801 was expected to enhance neurite outgrowth and to better monitor this effect a Casp-2 inhibitor plus CNTF were used to prevent RGC apoptosis. The Casp-2 inhibitor is a specific and irreversible inhibitor of caspase-2 (see instruction of R&D Systems, www.rndsystems.com/pdf/fmk003.pdf). It is also cell permeable and therefore does not require a transfection agent (Lipofectamine), as does siRTP801. CNTF enhances RGC survival but also stimulates neurite outgrowth (33,56).

To test the functional effect of siRTP801 on neurite length, RGC cultures were treated with either siRTP801, siRTP801 and CNTF or siRTP801,CNTF and Casp-2 inhibitor. CNTF was used as positive control whereas Lipofectamine was used as a transfection control. An untreated group was included as negative control.

5.1.3 RGC Survival In Vitro

Treating retinal cultures with CNTF enhanced RGC survival rates whereas treatment with siRTP801 alone and in combination with CNTF and Casp-2 inhibitor had lower survival rates. CNTF and siRTP801 treatment had a greater effect on RGC survival than did siRTP801 alone, however this effect was not as great as CNTF treatment alone. It seems that siRTP801 does not

have a marked effect on RGC survival, which was expected. Inhibiting the mTOR pathway appeared to promote neurite outgrowth rather than cell survival. The treatment that contained Casp-2 inhibitor in addition to siRTP801 and CNTF had the lowest survival rate compared to the other treatment groups, which was unexpected as Casp-2 inhibitor and CNTF both prevent apoptosis (4,33). The Casp-2 inhibitor was added one day after RGC had been cultured. During that time RGC may have already started to die. Therefore, Casp-2 inhibitor might have been less effective at this point. However, CNTF was still present in this treatment group but the survival rate is still lower that treatment with siRTP801 and CNTF. This could mean that Casp-2 inhibitor decreased RGC survival when added later than a few hours after culturing, it has some adverse effects on CNTF. Nevertheless, it needs to be emphasised that these experiments have been repeated only two times so no definitive conclusions can be drawn from that. An experiment where Casp-2 inhibitor is added to the RGC culture immediately after culturing and a day after culturing could be carried out to optimise how the inhibitor acts on RGC. Also, RGC could be treated with Casp-2 inhibitor and CNTF together to determine how those two reagents interact with each other in terms of RGC survival. In addition, when using a combinational treatment the dose of each treatment may need to be altered accordingly to have a synergistic effect.

5.1.4 Neurite Outgrowth In Vitro

Treatment with CNTF generated the highest number of βIII-tubulin positive RGC with neurites compared to other treatment groups. The siRTP801, CNTF and Casp-2 inhibitor and the siRTP801 plus CNTF treatments both enhanced the number of βIII-tubulin positive RGC with neurites. siRTP801 treatment alone had a minimal effect on neurite outgrowth compared to the other treatment groups.

CNTF induces neurite outgrowth in RGC (33), whereas siRTP801 did not. However, this might be because the concentration of siRTP801 was too high and inhibited neurite outgrowth. This could explain why there were more βIII-tubulin positive RGC with neurites when the RGC culture was treated with CNTF alone than with siRTP801+CNTF and why the fewest βIII-tubulin positive RGC with neurites were found in the siRTP801 treatment group. Casp-2 inhibitor does not have a documented effect on neurite outgrowth. This is also demonstrated by the data in Figure 7 where there is no difference between siRTP801+CNTF and siRTP801+CNTF+Casp-2 inhibitor treatment groups.

5.1.5 Mean Length of Longest Neurite In Vitro

The treatment groups that contained siRTP801 enhanced neurite length the most compared to the untreated controls, Lipofectamine or CNTF treatment groups. Although CNTF greatly enhanced RGC survival and the number of neurites it enhanced neurite length relatively little. All the treatment groups that contained siRTP801 did not enhance RGC survival. In addition, treatment groups with siRTP801 that also contained CNTF increased the number of

RGC with neurites but not as much as CNTF alone. Treatment with siRTP801 increased neurite length more than treatment with CNTF. The results indicate that siRTP801 does not act on RGC survival and is not as effective as CNTF in inducing neurite outgrowth. However, once a neurite has grown, treatment with siRTP801 seems to enhance neurite length. CNTF and siRTP801 together enhance neurite length more than on its own, which indicates that these two reagents act together to increase neurite length. Casp-2 inhibitor had no effect on RGC survival or number of RGC with neurites. Although the treatment group siRTP801+CNTF+Casp-2 inhibitor had fewer cells that survived, those RGC that did survive had the most increased neurite length out of all treatment groups. This might be because the Casp-2 inhibitor only prevents cell death when RGC are primed by neurotrophic factors and able to grow long neurites. Overall, siRTP801 does not enhance RGC survival or the number of RGC with neurites, but it seems to increase neurite length, which is an important factor for CNS regeneration. Especially in combination with CNTF and Casp-2 inhibitor, siRTP801 greatly enhanced neurite length.

5.1.6 Future Work for In Vitro Experiments

Although the generated data seems promising as treatment with siRTP801 enhanced neurite length, to fully come to a conclusion the experiments need to be repeated at least once more so statistical significance can be assessed. It would also be interesting to see the effect on RGC when treated with Casp-2 inhibitor on its own or in combination with CNTF and whether the time that this Casp-2 inhibitor is added influences RGC survival.

Even though a functional effect could be detected when RGC were transfected with siRTP801, to confirm RGC transfection efficiency, siRTP801 could be fluorescently tagged.

To establish whether the gene knock down has been successful, western blot could be carried out to determine the presence of RTP801 or qPCR to check whether the mRNA for RTP801 is still present.

Also, no specific test to determine apoptosis, such as the terminal deoxynucleotidyl transferase-mediated biotinylated UTP nick end labeling (TUNEL) staining was done. It would be good to know how many RGC were dying when treated with the Casp-2 inhibitor and in combination with siRTP801 and CNTF and when it would be best to treat RGC with Casp-2 inhibitor.

During the analysis for this study each well was divided into 9 squares and one picture was taken in the centre of each square. The cells sometimes cluster in certain areas of the culture well and if more pictures in one square had been taken, it would have generated more representative results.

5.2 *In Vivo* Studies

5.2.1 The Effect of siRTP801 and siCasp-2

Animals from the experimental and control groups received bilateral ONC and lens injury; the experimental group received ivit injections of siRTP801 and siCasp-2, the control group received equivalent injections of siEGFP. Treatment with siRTP801 and siCasp-2 enhanced RGC axon number proximal to the site of the ONC (the measure of RGC survival) more than

siEGFP. This was expected as another study had demonstrated that treatment with siCasp-2 induces survival of RGC *in* vivo (4).

The number of re-generating axons distal to the site of the ONC in the experimental and control group showed only slight differences, as the number of re-generating axons in the control group was high. This might be because both groups received a lens injury that causes inflammation and the release of neurotrophic factors. Studies have shown that inflammatory agents stimulate axon regeneration (27,29,32). The fact that the number of re-generating axons was so high in the control group makes the regenerative effect of siRTP801 difficult to assess. Nevertheless, a slightly higher number of axons were present at the most distal points to the site of ONC whereas slightly fewer axons were present closer to the site of the ONC when treated with siRTP801 and siCasp-2 compared to siEGFP. This indicates that despite fewer axons regenerating close to the distal site of the ONC, more axons that do regenerate grow longer distances when treated with siRTP801 and siCasp-2. These results are supported by the data generated in the *in vitro* experiment. Treating RGC with siRTP801 did not affect the survival rate or the number of RGC with axons but it affected the distance the axons regenerate.

However, due to the variability in response between animals, more animals are needed to confirm this data. In addition to that, the number of re-generating axons in the ON from the second eye of the examined animals should be quantified. Also, some of the animals developed cataracts (the measure of lens injury) but this was not documented for individual animals. The animals that had a cataract might have had a stronger inflammatory

reaction, which means that the axon regeneration could have been stronger compared to the animals without the cataracts. For the next study this should be documented and considered when doing the analysis.

For further details on RGC survival the retina containing RGC could be immunostained and quantified.

Overall, no definite conclusion can be made from this data but there is certainly a trend towards long distance axon regeneration initiated by siRTP801 transfection. Further experiments need to be carried out to confirm this hypothesis.

UNIVERSITY OF BIRMINGHAM

THE ROLE OF Fn14 AND TWEAK IN THE DEVELOPMENT AND RESOLUTION OF LIVER FIBROSIS

by

Annika Wilhelm

A thesis submitted to the University of Birmingham
in partial fulfilment of the requirements for the
award of the Master of Research

Centre for Liver Research
Institute of Biomedical Research
School of Immunity and Infection
College of Medical and Dental Sciences
University of Birmingham
August 2011

ABSTRACT

Hepatic fibrosis and its end stage cirrhosis are a major health burden worldwide caused by sustained accumulation of extracellular matrix (ECM). Cell therapy with mesenchymal stem cells (MSC) could be a promising approach to treat hepatic fibrosis and cirrhosis. Tumour necrosis factor-like weak inducer of apoptosis (TWEAK) and its receptor fibroblast growth factor-inducible 14 (Fn14) have been associated with modulating cell proliferation, differentiation, death and inflammation. Fn14 is highly up-regulated in the injured liver. Therefore, it would be important to understand how TWEAK-dependent Fn14 signalling affects MSC. Herein we present evidence that unstimulated MSC express Fn14. Fn14 expression decreases in adipogenic cultures and stimulation with TWEAK did not seem to affect adipogenesis. A single experiment in addition to literature suggests that TWEAK might influence MSC survival, which we may investigate in the future. We further report high Fn14 expression on hepatic stellate cells (HSC), the main source of ECM. However only one donor was investigated and therefore we need to carry out more experiments to consolidate these results. In conclusion, mesenchymal cells seem to express Fn14 but how TWEAK-dependent Fn14 signalling affects these cells is still inconclusive.

ACKNOWLEDGEMENTS

I would like to thank my principal supervisor Dr Simon Afford for his great advice and support throughout my project. The guidance, knowledge and moral support of my second supervisor Dr Victoria Aldridge have been invaluable during this project, for which I am extremely grateful.

Amongst my fellow postgraduate students I would like to thank Ricky Harminder Bhogal for his expertise in the 4-Colour Apoptosis/Necrosis/ROS production/Autophagy assay. I would also like to thank the rest of the Liver Research Group for their support and assistance.

TABLE OF CONTENTS

1. INTRODUCTION

1.1 General Introduction to Fibrosis

Fibrosis is a natural wound-healing response that involves regulation of scar formation (fibrogenesis) and degradation (fibrolysis) to acute or chronic injury to the liver. Fibrosis during acute injury is transient and reversible but the sustained signals during chronic injury lead to a several-fold increase in production and deposition of extracellular matrix (ECM) resulting in fibrosis (57). Not only the quantity of ECM but also the composition changes in the fibrotic liver. In the normal liver, the space of Disse contains mainly collagens type IV and VI but during fibrogenesis an increased deposition of collagens type I and III occurs (58). Hepatic stellate cells (HSC) are the main cellular source of ECM in hepatic fibrosis. In a healthy liver, HSC store lipid-soluble vitamin A metabolites (retinoids) (59) and reside in the space of Disse. However, following liver damage, HSC become active, loose their vitamin A storing capacity, start expressing α-smooth muscle actin (α-SMA), and transdifferentiate into myofibroblast-like cells with ECM secreting capacity (57,60,61) (Figure 1). Transforming growth factor-β (TGF-β) has been demonstrated to be the key mediator in activating HSC (62). Animal models have shown that inhibiting TGF-β, significantly decreases fibrosis (63). Nevertheless it has recently become clear that not all fibrogenic cells in the liver originate from HSC. Various research groups have demonstrated that portal fibroblasts (64), circulating fibrocytes (65) and bone marrow (66) can also contribute to liver fibrosis (Figure 2).

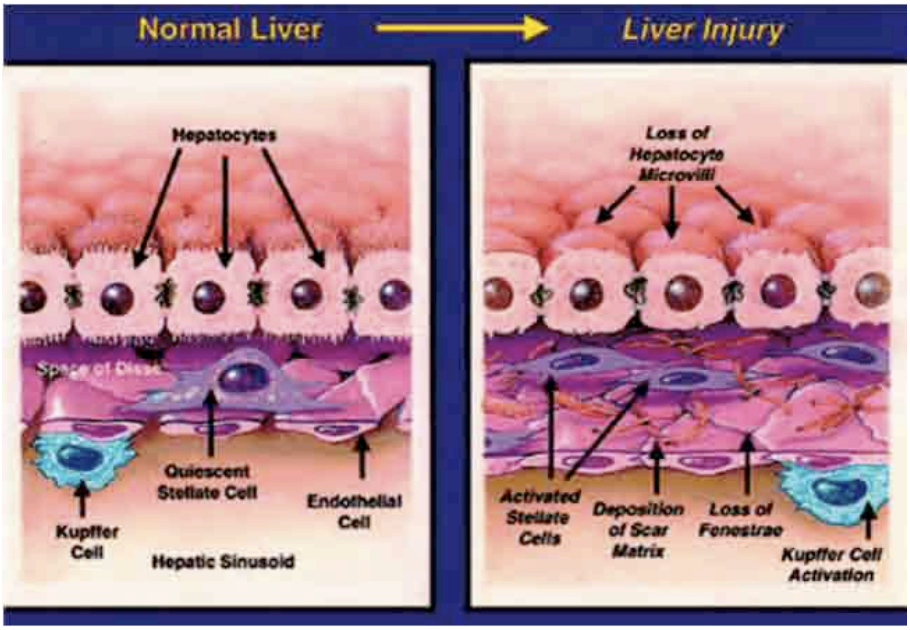

Fig 1. In a normal liver HSC reside in the subendothelial space of Disse. As a result of liver damage, HSC transdifferentiate into proliferative myofibroblasts that secrete ECM. Continues accumulation of ECM leads to liver fibrosis and eventually to cirrhosis. (Source of image 68)

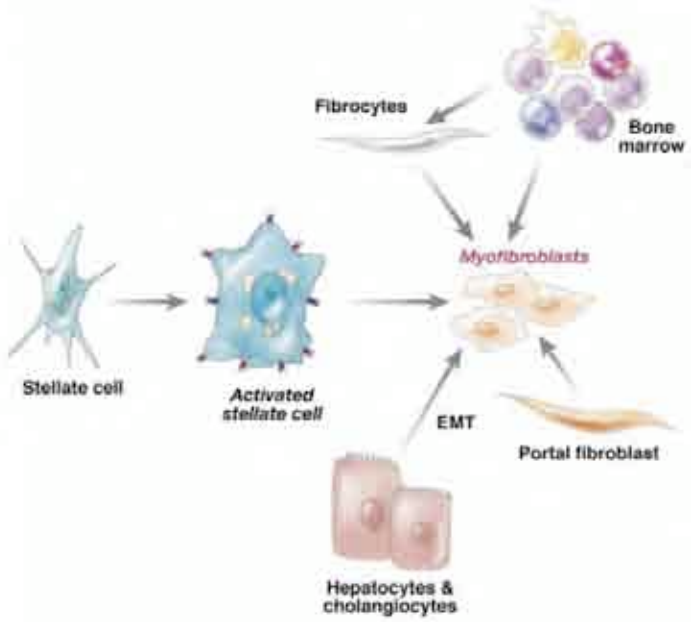

Fig 2. Although it was believed that all ECM-secreting myofibroblasts originate from HSC evidence suggest that portal fibroblasts, bone marrow, circulating fibrocytes and epithelial-mesenchymal cell transition (67) can also transdifferentiate into myofibroblasts (Source of image 69)

1.2 Cause and Treatment of Hepatic Fibrosis

Hepatic fibrosis and its most advanced stage, cirrhosis, can be caused by a number of factors including chronic infections with hepatitis B or C viruses, non-alcoholic steatohepatitis, toxic damage through long-term alcohol abuse and parasitemia (57). Cirrhosis is associated with an increased risk of liver failure and hepatocellular carcinoma (HCC). It represents a substantial health burden worldwide. In the UK over 4000 people die from cirrhosis every year and approximately 700 people have to have a liver transplant in order to survive (http://www.nhs.uk/conditions/Cirrhosis/Pages/Introduction.aspx).

A major issue with liver transplants are that donor livers are limited and patients have to take toxic, immunosuppressive medications for the rest of their life. However, new evidence suggests that even advanced fibrosis can be reversible (70,71) and therefore novel strategies to treat fibrosis and cirrhosis should be investigated. Cell therapy with hepatocytes, embryonic stem cell derived hepatocytes or mesenchymal progenitor cells shows promising results. Preventing accumulation of ECM *via* blocking activation of HSC is another strategy with potential.

1.3 Mesenchymal Progenitor Cells

Mesenchymal progenitor cells (MPC) are nonhaematopoietic multipotent cells that can differentiate into mesenchymal and nonmesenchymal lineages. MPC can be isolated from various tissues in the human body. One of the best studied MPC are mesenchymal stem cells (MSC) that can be isolated from bone marrow and other tissues such as muscle and fat. Bone marrow derived

MSC have been successfully used in several clinical trials for therapeutic application in patients with cirrhosis (72-74). Another type of MPC that are also of interest in the pathogenesis of cirrhosis are HSC, the resident cells of the liver. As mentioned above, it is believed that they are the main source of ECM in fibrogenesis. Therefore inhibiting HSC activation or causing apoptosis of active HSC would provide another possible treatment option for fibrosis.

1.4 MSC as Therapeutics for Cirrhosis

1.4.1 MSC Can Modulate the Immune System

MSC have been demonstrated to be an appealing source for cellular therapy and tissue engineering. The benefits of using MSC for therapeutic treatment include easy isolation and cultivation, high expansion potential and a stable phenotype (75,76).

MSC in their undifferentiated state have an anti-inflammatory effect (77) and as inflammation often precedes fibrosis, this could be an important attribute of MSC for cell therapy of fibrosis. The precise mechanisms by which MSC exert their immunosuppressive properties are still unclear but the production of various growth factors, cytokines and other signalling molecules may be involved (77). Studies have shown that during inflammation, pro-inflammatory cytokines such as tumour necrosis factor-α (TNF-α) and interleukin-1 (IL-1) are released. One study for example demonstrated that MSC can down-regulate inflammatory responses by secreting IL-1 receptor antagonists and upregulate anti-inflammatory cytokines such as IL-10 (78). Another study has shown that MSC can express high levels of inducible nitric-oxide synthase

(iNOS) and chemokines that are essential for immunosuppression (79). It is also believed that MSC supress inflammatory responses *via* cell-to-cell contact (80).

Even though the precise mechanisms by which MSC exert their immunosuppressive activity are still lacking, MSC have been used clinically for over a decade now to treat life-threatening graft-versus-host disease (GvHD). Evidence suggests that MSC inhibit T cell reactivity from the donor liver to histocompatibility antigens of the normal tissues of the recipient during the treatment of GvHD (76).

Besides the ability of MSC to modulate the immune system, they can also avoid recognition of another host's immune system. MSC lack for example major histocompatibility complex (MHC) class II to avoid recognition by CD4+ T cells (81). This is another benefit of MSC for cell therapy as it is more likely that allogeneic cells will be used to repair and replace damaged tissue. Compared to other cells, MSC are not recognised by the recipient's immune system as foreign and removed by immunocytes.

1.4.2 MSC Contribute to Liver Repair

The ability of MSC to modulate and evade the immune system is not the only therapeutic advantage that has been reported. Indeed as well as being capable of differentiating into cells from the mesenchymal lineage (82), MSC have been demonstrated to be capable of differentiating into hepatocyte-like

cells *in vitro*. These cells had functional characteristics of hepatocytes including albumin production, glycogen storage and urea secretion (83). However, when human MSC were directly injected into immunosuppressed rats with injured liver parenchyma, the differentiation efficiency into hepatocyte-like cells was very low (84). These results were also confirmed by another study using immunosuppressed mice (85). To avoid low differentiation efficiency *in vivo* MSC could be pre-differentiated before transplantation.

Another therapeutic advantage that has been attributed to MSC is preventing apoptosis and stimulating proliferation of hepatocytes in injured livers (86). In a rat model of D-galactosamine-induced fulminant hepatic failure (FHF), secreted factors from MSC significantly reduced rat mortality, decreased hepatocellular apoptosis up to 90% and enhanced hepatocyte proliferation (86). Furthermore, it has been demonstrated that MSC-derived molecules can reduce collagen secretion and proliferation of activated HSC (75). Also, animal and clinical trials showed that administration of MSC can decrease collagen accumulation in fibrotic livers and improve liver function (87-89).

1.4.3 Mesenchymal Stem Cells in Pathogenesis of Cirrhosis

It has recently been demonstrated in mice and human that bone marrow-derived cells can contribute to the myofibroblast population in fibrotic liver. This was discovered when a female patient that received a bone marrow transplant from a male donor (Y-chromosome) subsequently developed cirrhosis (66). The patient's liver contained 12.4% of Y-chromosome positive

myofibroblasts, which indicated that these myofibroblasts were of bone marrow origin (66). Following this, a mouse model was used in which female mice underwent bone marrow transplantation from a male donor followed by treatment with carbon tetrachloride (CCl_4) to induce liver fibrosis. This study demonstrated that 70% of myofibroblasts were of bone marrow origin (90). This outcome was also repeated in a bile duct ligation (BDL) mouse model of fibrosis (65). Transplantation of male MSC and female haematopoietic stem cells or vice versa into female mice confirmed that the myofibroblast population were of MSC and not haematopoietic stem cell origin (90). However it was not determined whether MSC immediately differentiate into myofibroblasts or whether they require transition through another cell type such as HSC (90).

The characteristics of MSC mentioned above are ideal for cell therapy to treat fibrosis and cirrhosis. MSC could be transplanted into the fibrotic liver to avoid liver transplantation. However, some doubts about their therapeutic effects of MSC for liver fibrosis remain, as MSC can also differentiate into myofibroblasts.

1.5 TNF Superfamily

Cytokines and their receptors that are of potential interest for fibrogenesis, belong to the tumour necrosis factor (TNF) superfamily. One of the best-known cytokines of this family is TNF-α, which is a central player in inflammation. TNF-α is an important regulator of the nuclear factor kappa light chain enhancer of activated B cells (NF-κB) pathway that is involved in

controlling expression of genes that influence inflammation, proliferation, differentiation and cell migration (91).

MSC can migrate out of the bone marrow to sites of injury and inflammation, which can be enhanced by TNF-α and it has been demonstrated that TNF-α enhances the proliferative potential of MSC (92). In addition, TNF-α is involved in the immunosuppressive ability of MSC *in vivo* and *in vitro* (80) and can increase adhesion of MSC to hepatic endothelium (unpublished data from V. Aldridge). Furthermore, Kupffer cells, the resident liver macrophages, secret TNF-α during fibrosis, which has been shown to have an anti-apoptotic effect on activated HSC (93). These studies show that the influence of TNF-α plays a critical part in modulating fibrosis and influence the physiological properties of mesenchymal progenitor cells.

1.5.1 TWEAK and its Receptor Fn14

The TNF and TNF receptor (TNFR) superfamily has several members and part of this superfamily is the recently identified cytokine, TNF-like weak inducer of apoptosis (TWEAK) and its receptor FGF-inducible molecule-14 (Fn14). TWEAK is synthesised as type II-transmembrane protein that can be proteolytically cleaved to function primarily as a soluble cytokine (94). It is highly expressed by immunocytes and has been detected in tissues with acute injury and inflammation (95,96).

TWEAK's receptor, Fn14 is the smallest receptor of the TNFR superfamily. It is a 14-kDa type I transmembrane receptor with only one cysteine-rich domain

at its extracellular ligand-binding region (97). In healthy tissue, Fn14 is expressed in low levels whereas high expression levels can be detected in tissues with inflammation. When Fn14 is up-regulated, it associates with TNF receptor associated factors (TRAFs) *via* its cytoplasmic domain and activates NF-κB (98). Compared to TNF-α, TWEAK induces a prolonged NF-κB activation (99). This indicates TWEAK's potent ability to contribute to inflammatory diseases. In addition, TWEAK-dependent Fn14 signalling has been shown to regulate several cellular processes including proliferation, differentiation, migration, angiogenesis, apoptosis and proinflammatory responses similar to its sibling TNF-α (100).

1.5.2 TWEAK-dependent Fn14 Signalling in Disease

Several studies in recent years have indicated that TWEAK-dependent Fn14 signalling has a role in the pathogenesis of inflammatory diseases. Those studies showed that overexpression of TWEAK in various tissues of mice can lead to profound dilated cardiomyopathy (101) skeletal muscle wasting (102) and breakdown of the blood-brain barrier (103). In addition, administration of TWEAK to normal mice led to features of inflammatory kidney disease (104). In contrast, other studies using TWEAK neutralising monoclonal antibodies (mAb) or Fn14 deficiency have shown to be beneficial during injury. Mouse models of human systemic lupus erythematosus (SLE) nephritis for example had decreased disease severity when they did not express *Fn14* or were treated with anti-TWEAK mAb (105).

Overall, these observations indicate that overactive TWEAK-dependent Fn14 signalling can be detrimental and that deficiency of TWEAK-dependent Fn14 signalling can be beneficial to pathological outcomes.

Although the activity of TWEAK is often associated with detrimental effects in inflammatory diseases, it has been reported that TWEAK's activity can also be beneficial. Two studies showed that TWEAK is a mitogen for liver progenitor cells, which indicates that TWEAK can be involved in liver regeneration (106,107). Fn14 is normally not detectable in a healthy liver, which mainly contains hepatocytes but becomes up-regulated in human hepatocellular carcinoma tissue (108). Also, Fn14 expression becomes up-regulated in hepatocytes of mice within 4 hours after a partial hepatectomy and during hepatocarcinogenesis compared to normal mouse livers (108). This implies that TWEAK and Fn14 have an important role during proliferation of hepatic epithelial cells and therefore liver regeneration. Furthermore, it has been suggested that Fn14 is not the only receptor for TWEAK (109). However, with an *Fn14*-null mouse model Jakubowski *et al.* demonstrated that TWEAK's mitogenic effect on liver progenitor cells is Fn14 dependent (107). In addition, it has been demonstrated that MPC also express Fn14 (110).

TWEAK can bind to several other progenitor cells, including MSC and muscle myoblasts (110). Muscle myoblasts exhibited increased proliferation when stimulated with TWEAK and decreased proliferation when treated with an anti-Fn14 blocking antibody *in vitro*. Also, *Fn14*-null mice showed delayed muscle

regeneration and inflammatory responses (110). These results identify TWEAK as new modulator of regenerative myogenesis. Adipose tissue-derived mesenchymal stem cells (AMNC) also express TWEAK and Fn14 and their interaction affects differentiation into adipocytes (111). Research shows that Fn14 expression decreases when ADMC or MSC undergo adipogenesis. In accordance to that TWEAK has been demonstrated to inhibit adipogenesis and is present in immature adipose tissue but not in mature adipose tissue (111). Moreover, MSC were affected by TWEAK stimulation, showing an up-regulation of NF-κB and expression of pro-survival, pro-proliferative and cell adhesion genes (110).

TWEAK-dependent Fn14 signalling is involved in inflammation and in progenitor proliferation and differentiation. Understanding how Fn14 signalling influences MPC proliferation and differentiation would be a great success in the progress of cell therapy for fibrosis.

2. OBJECTIVES

Despite advances in understanding the pathology of fibrosis, there is limited therapy available. Cell therapy with MPC could be a promising approach to find treatment for hepatic fibrosis and cirrhosis. MSC that have been demonstrated to modulate the immune system and potentially contribute to liver repair are prospective new therapeutic agents to target liver fibrosis. However, MSC might also contribute to the pathogenesis of fibrosis by differentiating into myofibroblasts. Therefore it is crucial to further investigate the basic biology of MSC and the behaviour of MSC when they are exposed to factors from microenvironment of a fibrotic liver. Furthermore finding a way to prevent activation or induce apoptosis of HSC would be another promising way to treat liver fibrosis. Recent studies have demonstrated the involvement of TWEAK-dependent Fn14 signalling in progenitor proliferation and differentiation. To investigate whether TWEAK-dependent Fn14 signalling affects MSC, we will carry out experiments to test Fn14 and TWEAK expression on MSC, the effect of adipogenesis on Fn14 expression and the influence of TWEAK on adipogenesis and MSC survival. In addition, we will investigate Fn14 expression on HSC.

3. MATERIALS AND METHODS

Unless otherwise stated human MSC and appropriate media were obtained from LONZA (Wockingham, UK) and human HSC and appropriate media were obtained from TCS Cellworks (Buckingham, UK).

3.1 Setting up Human MPC Cultures

For long-term storage, MPC were kept in liquid nitrogen (-150ºC). To set up MPC cultures, cryovials were removed from storage and disinfected with 70% ethanol before opening. In a sterile environment cells where thawed by adding room temperature, sterile phosphate buffer saline (PBS). Thawed cell were transferred to 25ml tube containing 25ml sterile PBS and centrifuged for 5 minutes at 726g to pellet cells. The pellet was resuspended in the appropriate medium for each cell type (Table 1) by gently pipetting up and down. For MSC, cell suspension was transferred to a 175cm^2 culture flask (BD Falcon) containing 25ml supplemented MSCBM (Table 1). HSC suspension was transferred to a 75cm^2 culture flask (Corning) pre-coated with poly-L-lysine (0.1 mg/ml in TC grade distilled water; Sigma, Poole, UK) containing 10ml HSC medium (ScienCell, Buckingham, UK) (Table 1). Flasks were rocked to distribute cells over flask surface and incubated at 37ºC 5%CO_2 in a humidified environment for at least 12 hours.

Type of Cells	Medium	Volume (ml)
MSC	Mesenchymal Stem Cell Basal Medium (MSCBM) - Mesenchymal Growth Supplement (MCGS) - L-Glutamine - GA-1000	440 50 10 0.5
HSC	SteCM Stellate Cell Medium	-

Table 1. Media for MPC

3.2 Maintenance of Human MPC

3.2.1 Passaging MPC

In a sterile environment, 10 or 15ml medium (depending on whether it was a 75 or 175cm^2 culture flask) was removed and transferred into a 25ml tube. The cells were rinsed with sterile PBS, which was then discarded and 5 or 10 ml TrypLE (Gibco) added. Flaks were gently tapped to detach cells from the plastic and viewed under a microscope to ensure detachment. The medium retained at the beginning was added to the flask to inactivate TrypLE. The cell solution was then transferred to a 25ml tube and centrifuged for 5 minutes at 726g to pellet the cells. The cell pellet was resuspended in the appropriate medium (Table 1) by gently pipetting up and down and transferred into new flasks containing pre-warmed MSCBM (for MSC) or HSC medium. Flasks were rocked to distribute cells over flask surface and incubated at 37ºC 5%CO_2 in a humidified environment. Medium was changed every 2-3 days completely. Cells were passaged when reaching around 85% confluency.

3.2.2 Cryopreservation for MPC

Cells were detached from flask as described in section 3.2.1. After centrifugation supernatant was removed and cells were resuspended in 3ml of cryopreservation medium (5%DMSO in foetal calf serum (FCS)). 500,000 to 2,000,000 cells per ml were added per cryovial and the vials were stored in a "Mr Frosty" containing 250ml propan-2-ol at -80ºC for at least 24 hours. For long-term storage, the cryovials were stored at -150ºC in liquid nitrogen.

3.3 Flow Cytometry

3.3.1 Cell Surface Flow Cytometry

Depending on the experiment, cells were either treated 24 hours in advance to the experiment or left untreated. MSC were treated with TNF-α (1:1000, 10µg/ml) (Peprotech, London, UK) and HSC were treated with human TGF-β (1:1000, 10µg/ml) (Peprotech, London UK). Cells were detached from the flask as described in in section 3.2.1. After centrifugation, the supernatant was removed and cells were resuspended in FACS buffer (10% FCS in sterile PBS). 100µl of cell suspension was added to each FACS tube. Primary antibodies for Fn14/TWEAK staining or conjugated-antibodies for MSC markers (Table 2) were added to individual FACS tubes and incubated at 4ºC for 30 minutes with agitation in the dark. After 30 minutes, cells were washed twice with FACS buffer and centrifuged for 5 minutes at 726g. FACS tubes with antibodies against MSC marker were immediately analysed on a flow cytometer. During Fn14/TWEAK staining, the supernatant was removed and

100µl of secondary antibody Alexa Fluor 488 (1:250, goat anti-mouse IgG, Invitrogen, Paisley, UK) diluted in FACS buffer was added to each FACS tube. Cells were then incubated at 4ºC for 30 minutes with agitation in the dark. After 30 minutes, cells were washed twice with FACS buffer and centrifuged for 5 minutes at 726g. The supernatant was removed and cells were resuspended in 500µl FACS buffer and analysed immediately using a CyAn flow cytometry machine (Dako) and Summit software Version 3. Experiments were repeated with multiple MSC donors.

	Primary Anitbody	Dilution	Stock concentration	Supplier
Fn14 expression	Control	-	-	-
	IgG1*	1:50	300µg/ml	Gift from Biogen Idec Inc.
	Fn14*	1:50	370µg/ml	Gift from Biogen Idec Inc.
TWEAK expression	Control	-	-	-
	IgG2a*	1:50	398.5µg/ml	Gift from Biogen Idec Inc.
	TWEAK*	1:50	324µg/ml	Gift from Biogen Idec Inc.
MSC markers	Control	-	-	-
	CD73*	1:10	-	Miltenyi Biotec, Surrey
	CD90*	1:10	-	Miltenyi Biotec, Surrey
	CD105*	1:10	-	Miltenyi Biotec, Surrey
	Test-Mix*	1:10	-	Miltenyi Biotec, Surrey
	IgG-Mix*	1:10	-	Miltenyi Biotec, Surrey
* Mouse anti-human				

Table 2. Primary antibodies for Fn14 and TWEAK surface expression and antibodies from MSC Phenotyping Kit (Miltenyi Biotec, Surrey, UK; #130-095-198)

3.3.2 Intracellular Flow Cytometry for TWEAK

For intracellular staining, cells were removed from flask as described in section 3.2.1 and resuspended in 2% paraformaldehyde (PFA) in PBS. Cells were then incubated for 20 minutes at 4ºC. After 20 minutes, cells were washed with permeabilisation buffer (1X BD Perm/Wash buffer in hH_2O, BD Biosciences, Swindon, UK) for 15 minutes and centrifuged for 5 minutes at 726g twice in 500µl permeabilisation buffer. Cell pellet was resuspended in 300µl permeabilisation buffer and 100µl of cell suspension was added to each FACS tube. Cells were then stained according to the protocol in section 3.3.1 starting from the step where primary antibodies (Table 2, TWEAK expression) are added. Instead of FACS buffer, permeabilisation buffer was used throughout the protocol except at the final step when 500µl FACS buffer was added.

3.4 Adipogenic Differentiation of MSC

MSC were differentiated into adipocytes using hMSC adipogenic differentiation BulletKit according to the manufacturers protocol (LONZA, Wockingham, UK, PT-3004). Briefly, $2x10^5$ cells were plated per well in a 6-well plate and incubated at 37ºC 5%CO_2 in a humidified environment until reaching 100% confluence. Once confluent, cells were treated with induction medium for 3 days and the maintenance medium for 2-3 days (Table 3). Controls were treated at the same schedule with either maintenance medium only or MSC medium only. This was repeated for 3 cycles and after

completion, cells were cultured for another 7 days in maintenance medium. Controls that had been treated with MSC medium only were continued to be treated with the same medium.

For a separate experiment, TWEAK protein (1:1000, 10µg/ml) (Gift from Biogen Idec Inc., Cambridge, USA) was added to the MSC culture at the beginning of each cycle.

At the end of each cycle, flow cytometry analyses for Fn14 expression and Oil Red O staining were carried out. In addition, MSC were observed through a microscope at twenty times magnification and photos were taken with a Canon EOS 40D.

	Content	Volume (ml)
Maintenance Medium	Adipogenic Maintenance Medium - h-Insulin - L-Glutamine - MCGS - GA-1000	170 2 4 20 0.2
Induction Medium	Adipogenic Induction Medium - h-Insulin - L-Glutamine - MCGS - Dexamethasone - Indomethacin - IBMX - GA-1000	170 2 4 20 1 0.4 0.2 0.2

Table 3. Media used for adipogenic differentiation of MSC

3.4.1 Oil Red O Staining

Oil Red O (Sigma-Aldrich) was prepared by adding 15ml of Oil Red O stock solution (0.25g Oil Red O in 50ml 100% Isopropanol) to 10ml of distilled (d) H_2O and incubated for 10 minutes at room temperature. The solution was then filtered two times through a filter paper (Whatman).

At the end of the differentiation protocol the cells were fixed in formal saline solution for 10 minutes and then washed twice with PBS. PBS was aspirated and 60% Isopropanol in dH_2O was added to wells for 5 minutes. The Isopropanol was then aspirated and cells were incubated at room temperature for 1 hour in freshly prepared Oil Red O. Oil Red O was removed and 60% Isopropanol was added and incubated for 5 minutes. The cells were then washed twice with dH_2O. Images were taken with a Canon EOS 40D.

For quantification, Oil Red O was solubilised by adding 500µl of 100% Isopropanol to each well and then incubated for 10 minutes on a plate shaker. 500µl of each well were evenly distributed between 5 wells of a 96-well plate and the released stain was quantified using a Synergy HT plate reader (BIO-TEK). Readings were taken at 520nm. 100% Isopropanol only was used to determine background staining.

3.5 4-Colour Apoptosis, Necrosis, ROS production, Autophagy Assay

The 4-colour assay was used to determine reactive oxygen species (ROS) production, autophagy, apoptosis and necrosis. To determine ROS production, the non-fluorescent substrate 2',7'-dichlorofluorescin-diacetate (H2DCF; Merck, Nottingham, UK) was used. H2DCF is cell permeable and once inside the cell it becomes trapped as a result of hydrolysis by intracellular esterases to 2',7'-dichlorofluorescin (DCF) (112). DCF then reacts with ROS leading to production of green fluorescence. Autophagy was determined with the autofluorescent compound monodansylcadaverine (MDC) (Fluka, Sigma-Aldrich) that labels autophagic vacuoles (113). Annexin-V (Molecular Probes, Paisley, UK) was used to detect apoptosis. When cells undergo apoptosis, phosphatidyl serine is translocated to the cell surface where Annexin-V will bind it with high affinity (114). 7-Amino-Actinomycin D (7-AAD, Molecular Probes, Paisley, UK) is a fluorescent compound that determines necrosis. 7-AAD can only enter a cell when the plasma membrane is disrupted but once inside a cell it binds with high affinity to DNA (115).

MSC were plated into 6-well plates and when 85% confluent MSC were treated with TWEAK (1:1000, 10µg/ml), TNF-α (1:1000, 10µg/ml) or left untreated. After 12 or 24 hours the medium was aspirated and 2ml HBSS -Ca^{2+}, -Mg^{2+} (Gibco) was added. 6µl of DCF and 1µl of MDC were added to each well and incubated at 37ºC for 30 minutes in the dark with agitation. The

wells were then treated with 2ml TrypLE at 37ºC for 5 minutes in the dark. To ensure all cells were detached TrypLE was gently pipetted up and down. Then 2ml of FCS was added to inactivate the TrypLE and the cell solution was transferred to a 15ml tube. The cells were washed in PBS and centrifuged at 726g for 5 minutes twice. PBS was removed and 100µl PBS was added and transferred into a FACS tube. 5µl Annexin-V and 2µl 7-AAD was added to each FACS tube and incubated for 15 minutes on ice. Next, 400µl PBS were added and the samples were immediately analysed by flow cytometry.

In order to compensate, one well was treated with each fluorescent substrate alone to avoid crossover of fluorophores. Approximately 10,000-gated cells were counted for each experiment.

3.6 Immunofluorescence

Cells were plated on sterile glass coverslips in 24-well plates. MSC were treated with TNF-α (1:1000, 10µg/ml) and HSC were treated with TGF-β (1:1000, 10µg/ml; both Peprotech, London UK). After 24 hours, the medium was aspirated and cells were fixed for 15 minutes in 4% PFA in PBS. After rinsing wells with PBS, 4 drops of Image-iT signal enhancer (Invitrogen) were applied and incubated for 30 minutes. Wells were rinsed with PBS and blocked with 10% goat serum (Vector Laboratories, Petersborough, UK) in PBS/0.3% TritonX (Sigma-Aldrich) for 10 minutes. Each well was then treated with primary antibodies (Table 2, Fn14 expression) at a 1:50 dilution in 10% goat serum in PBS/0.3% TritonX for 1 hour. After 1 hour, wells were washed 3

times for 10 minutes with PBS. The secondary antibody, Alexa Fluor 488 (goat anti-human IgG) was applied in a 1:500 dilution in 10% goat serum in PBS/0.3% TritonX and incubated for 1 hour in the dark. Wells were washed 3 times for 10 minutes with PBS, incubated with DAPI (Invitrogen) at a 1:5000 dilution in PBS for approximately one minute and then rinsed with PBS/0.1% TritonX. Fluoromount mounting medium (Dako) was used to mount coverslips and left to dry. Slides were then viewed with an epi-fluorescent microscope and Axiovision software was used to capture images (both Carl Zeiss MicroImaging, LLC, Thornwood, NY).

3.7 Statistical Analysis

If not stated otherwise an N value of 3 was obtained. The Student T Test was carried out and a P value of < 0.05 was considered as significant.

4. RESULTS

4.1 Characteristics of MSC

MSC have a fibroblast like appearance (Figure 3A) and can differentiate into various cell types including chondrocytes, osteocytes and adipocytes (previously performed by V. Aldridge). Flow cytometry analysis showed that MSC population was heterogeneous in size and granularity as shown with the forward and side scatter dot blot (Figure 3B). As expected the MSC marker kit showed that MSC were positive for CD73, CD90 and CD105 and negative for CD14, CD20, CD34 and CD45 (Figure 3C).

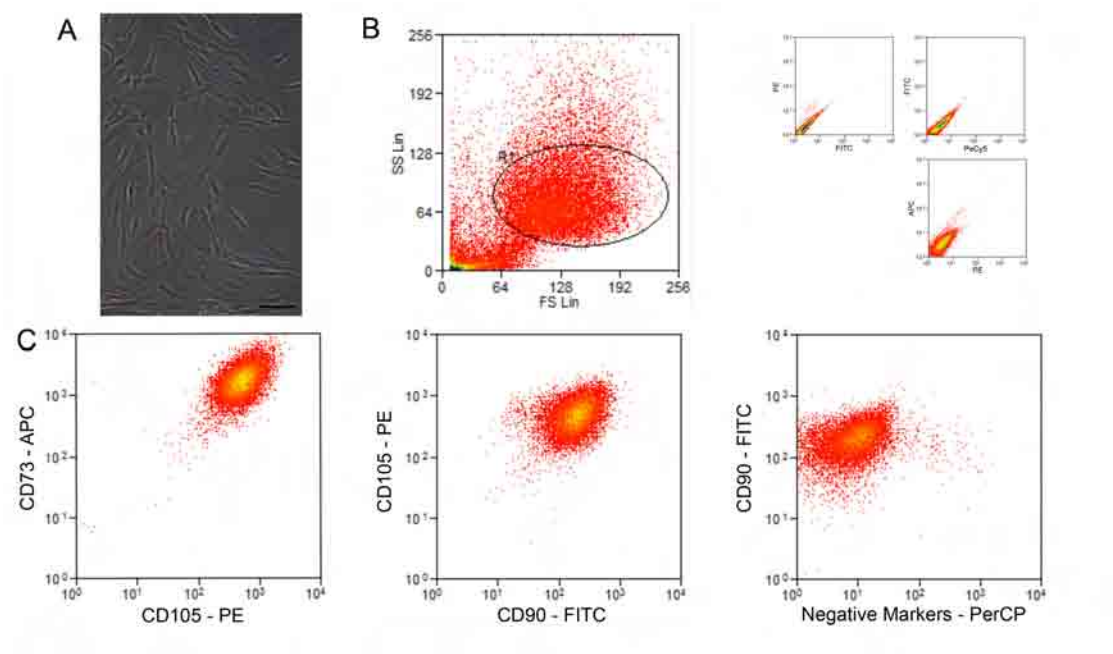

Figure 3. Morphology and expression of surface molecules Morphology of MSC, Scale bar 100µm (A) Forward versus side scatter with at least 10,000 gated events and isotype control (B) CD73+, CD90+ and 105+ cells and CD14-, CD20-, CD34- and CD45-cells (fluorescent dye PerCP) (C)

4.2 Expression of Fn14 on MSC

Flow cytometry was used to determine Fn14 expression on MSC. The pulse width was used to distinguish single cells from cell clumps or aggregates (Figure 4A). MSC were treated with TNF-α for 24 hours or left unstimulated. On average 93% of MSC expressed Fn14 and that slightly increased to an average of 98% with TNF-α stimulation (Figure 4B-C). The median fluorescent intensity (MFI) describes the number of receptors present per cell. On average a greater MFI was detected on TNF-α stimulated cells (71) versus unstimulated cells (50) but the increase was not statistically significant ($p > 0.05$) (Figure 4C). Fn14 expression was also detected with immunocytochemistry on unstimulated and TNF-α stimulated MSC (Figure 4D). The fluorescent staining appears to be stronger in TNF-α treated cells than unstimulated cells, which correlates with the MFI from flow cytometry (Figure 4C-D).

Overall, the percentage of unstimulated and TNF-α stimulated cells expressing Fn14 is very similar. However, it seems that cells that have been stimulated with TNF-α have slightly more Fn14 receptors on the cell surface than untreated MSC.

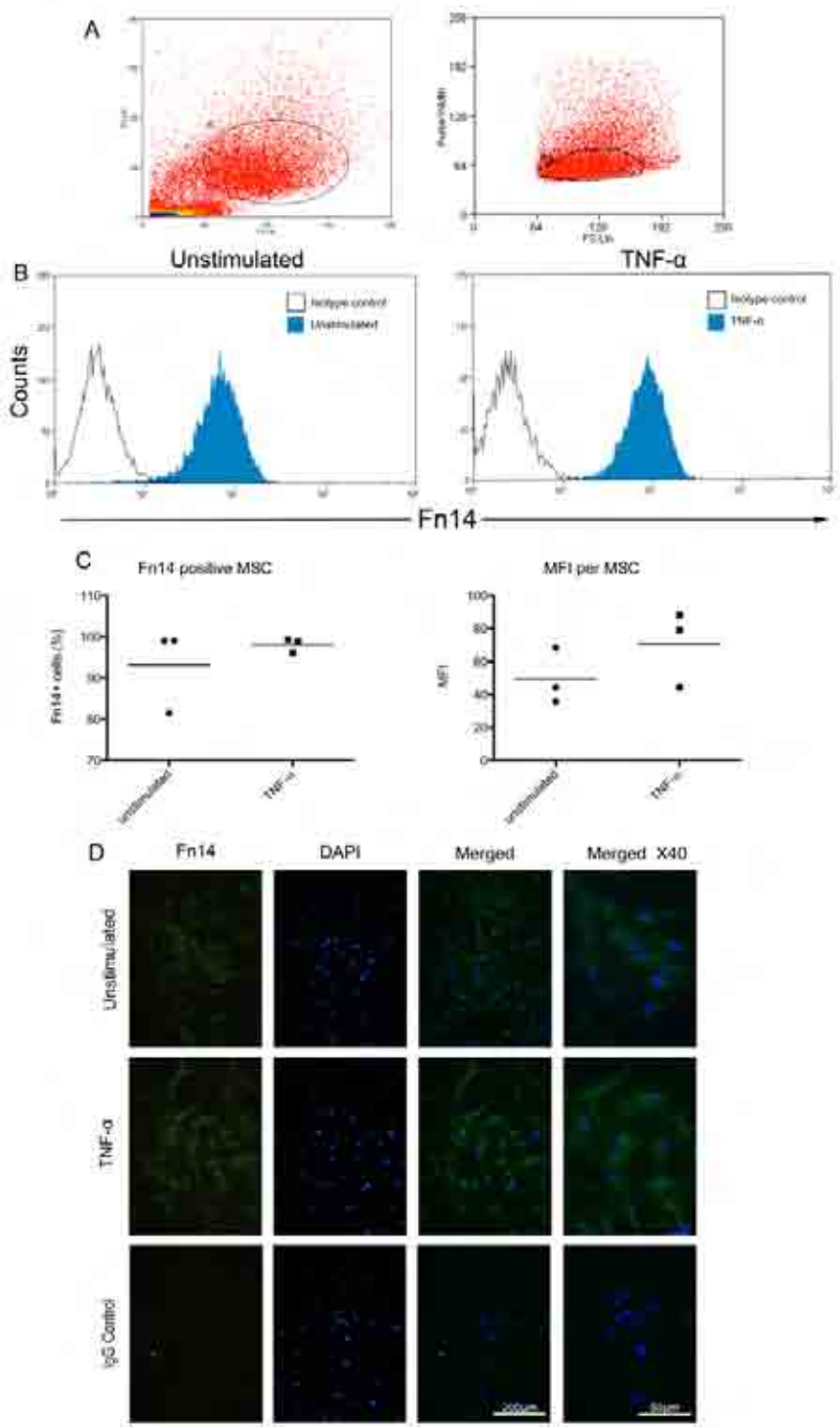

Fig 4. Fn14 expression on MSC. Forward versus side scatter with at least 10,000 gated events and pulse width (A) Flow cytometric analysis of Fn14 expression on unstimulated and TNF-α stimulated MSC (B) Percent of Fn14 positive cells and MFI of unstimulated and TNF-α stimulated MSC, each symbol represents an individual donor (C) Unstimulated and TNF-α stimulated MSC positive for Fn14 expression counterstained with DAPI. Scale bar, 200μm. Scale bar merged X40 50μm (D)

4.3 Expression of TWEAK on MSC

MSC were examined for TWEAK expression with flow cytometry (Figure 5). No TWEAK expression was detected on the cell surface of either unstimulated or TNF-α stimulated MSC (Figure 5A). Furthermore, no TWEAK expression was detected intracellularly in unstimulated MSC (Figure 5B).

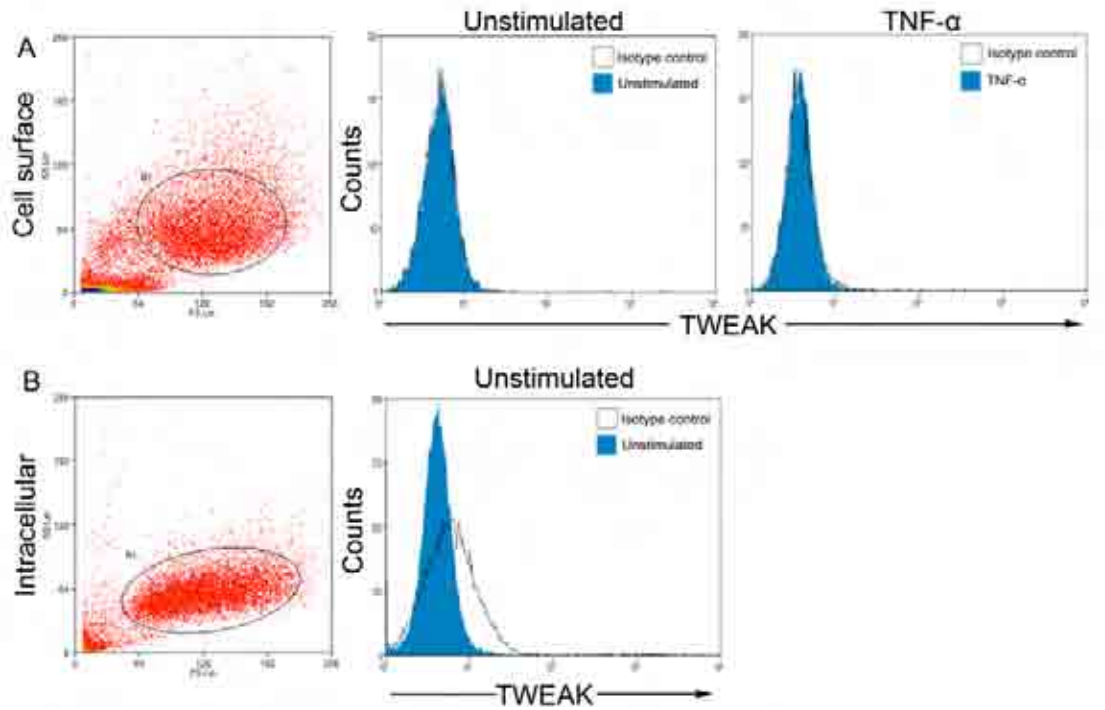

Fig 5. TWEAK expression on MSC. Forward versus side scatter with at least 10,000 gated events (A+B) Flow cytometric analysis of TWEAK expression on the cell surface of unstimulated and TNF-α stimulated MSC (A) Intracellular TWEAK expression of unstimulated and TNF-α stimulated MSC (B)

4.4 Fn14 Expression during Adipogenesis

To investigate whether differentiation of MSC affects Fn14 expression, MSC were differentiated over 3 weeks into adipocytes. Differentiation into adipocytes was confirmed by formation of cytoplasmic lipid vacuoles. Oil Red

O was used to stain lipid vacuoles red (Figure 6). Not all cells in the culture differentiated into adipocytes. Cells treated with MSC medium or Maintenance medium as a control did not change morphology and did not stain red with Oil Red O (Figure 6).

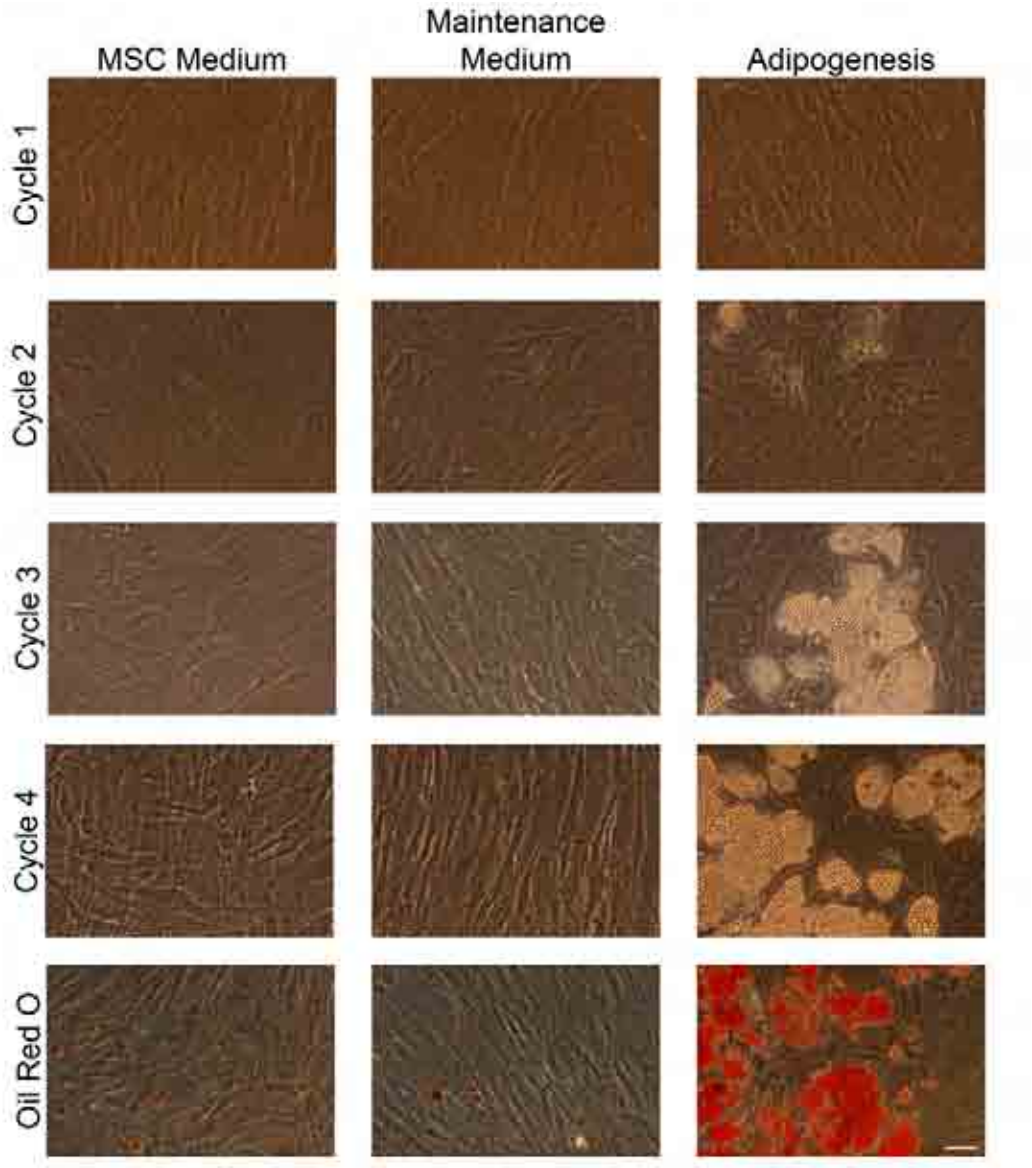

Fig 6. MSC differentiation into adipocytes. Induction and maintenance medium were used to induce adipogenesis in MSC. MSC medium and maintenance medium only were used as a control. Oil Red O staining confirmed cytoplasmic lipid vacuoles that form during adipogenesis. Scale bar 30µm

Flow cytometry was used to analyse the expression of Fn14 on MSC during the course of differentiation. MSC populations treated with MSC or maintenance medium remained heterogeneous in size and granularity as shown with the forward and side scatter dot blot (Figure 7A, insert). Differentiation of MSC into adipocytes resulted in greater variability in forward and side scatter properties (Figure 7A, insert).

After the first cycle (5 days in culture) the average Fn14 expression in MSC medium is 95%, in maintenance medium 91% and in adipogenesis medium 89%. After the second cycle (9 days in culture) the average Fn14 expression in MSC medium is 86%, in maintenance medium 53% and in adipogenesis medium 84%. After the third cycle (14 days in culture) the average Fn14 expression in MSC medium is 48%, in maintenance medium 20% and in adipogenesis medium 57%. After the forth and final cycle (21 days in culture) the average Fn14 expression in MSC medium is 22%, in maintenance medium 7% and in adipogenesis medium 48%. Average Fn14 expression decreases from the first to the final cycle by 41% in the adipogenic culture, 74% on cells treated with MSC medium and 84% on cells treated with maintenance medium (Figure 7).

The average MFI after the first cycle is 42 in MSC medium, 40 in maintenance medium and 43 in adipogenesis culture. After the second cycle the average MFI is 22 in MSC medium, 39 in maintenance medium and 43 in adipogenesis culture. After the third cycle the average MFI is 21 in MSC medium, 36 in maintenance medium and 21 in adipogenesis culture. After the

final cycle the average MFI is 29 in MSC medium, 48 in maintenance medium and 23 in adipogenesis culture. The MFI drops significantly ($p < 0.01$) from cycle 1 to cycle 3 when cells were treated with MSC medium or adipogenic medium but drops minimally when cells were treated with maintenance medium. Also the MFI rises in the final cycle in cultures with maintenance or adipogenic medium (Figure 7B). Overall, Fn14 expression decreased during adipogenesis but it cannot be said that this was as a result of adipogenic differentiation as both control groups also lost Fn14 expression.

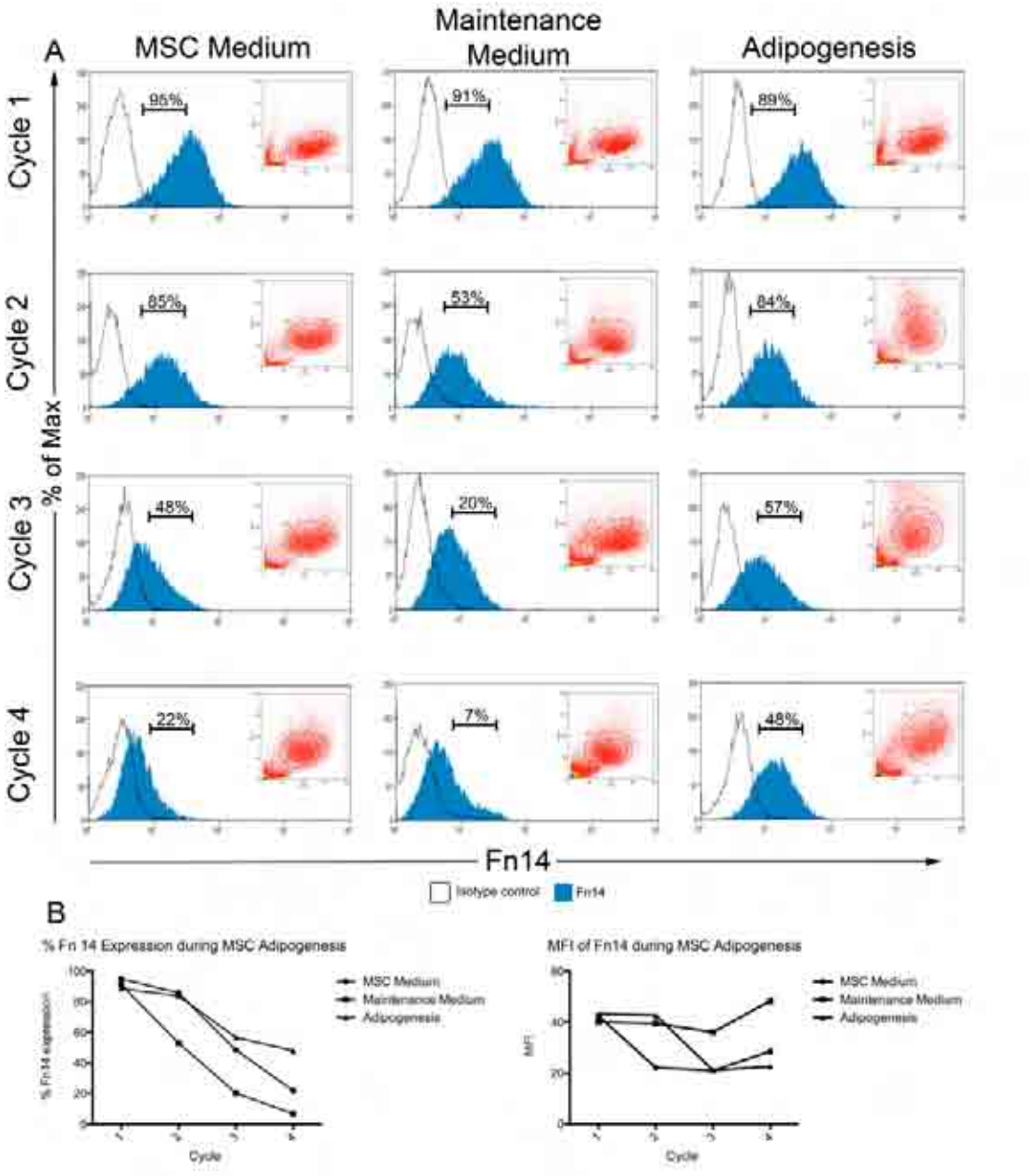

Fig 7. Fn14 expression during adipogenesis. Adipogenesis was induced by three cycles of induction and maintenance medium and then 7 more days in maintenance medium. MSC and maintenance media were used as a control. Flow cytometric analysis for F14 expression of MSC cultures in control media and during adipogenesis (A). Mean percentage of Fn14 positive cells and mean MFI during 4 cycles of adipogenesis (B) Each experiment was carried out in triplicate.

4.5 Effect of TWEAK on Adipogenesis

TWEAK has previously been demonstrated to interfere with adipogenic differentiation of adipose tissue derived mesenchymal cells (ADMC) (111). Therefore we decided to study the effects of TWEAK on MSC during adipogenesis. No morphological changes of cells were detected during adipogenesis compared to cells that were not stimulated with TWEAK (Figure 8A). An accumulation of cytoplasmic lipid vacuoles was detected and confirmed with Oil Red O staining in untreated and treated cultures (Figure 8A). Performing fat quantification by measuring the amount of Oil Red O stain in culture confirmed that TWEAK did not affect differentiation potential of MSC ($p > 0.05$) (Figure 8B). However, when MSC were treated with maintenance medium plus TWEAK the culture seemed to be more confluent than treatment with maintenance medium alone. This could indicate that TWEAK has an effect on proliferation on MSC but more experiments need to be carried out in order to confirm this hypothesis (Figure 8A).

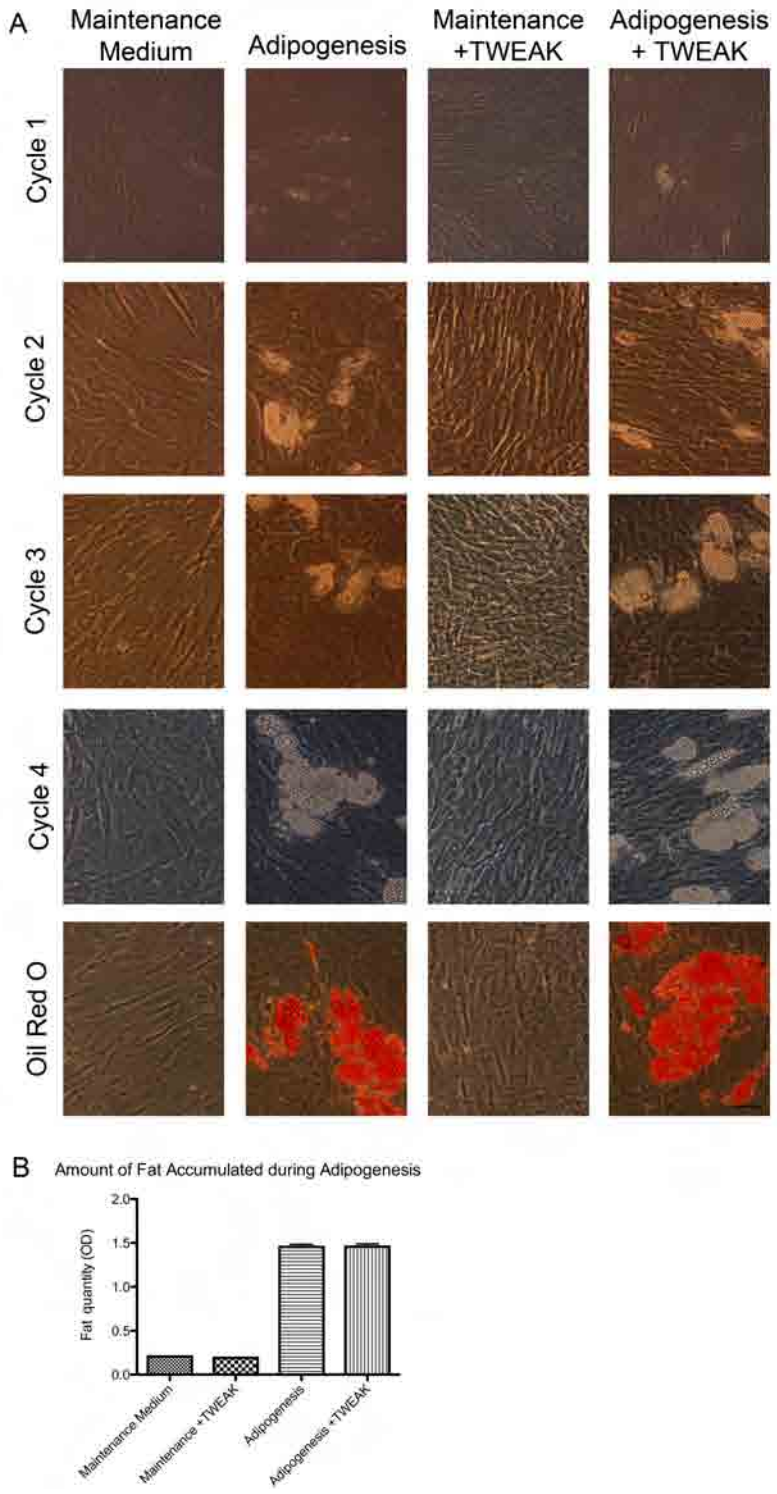

Fig 8. MSC differentiation into adipocytes in the presence of TWEAK. Induction and maintenance medium were used to induce adipogenesis in MSC with or without TWEAK. Maintenance medium were used as a control. Oil Red O staining confirmed cytoplasmic lipid vacuoles. Scale bar 30µm (A) Fat accumulation was measured with a plate reader at 520nm Values are means ± SEM. (B)

4.6 Effect of TWEAK on Apoptosis, Necrosis, ROS Production and Autophagy

To further investigate how TWEAK might influence MSC behaviour, a four-colour flow cytometry assay was carried out to detect apoptosis, necrosis, autophagy and ROS production. MSC were treated with TWEAK, TNF-α or left unstimulated for either 12 or 24 hours. After 12 or 24 hours of stimulation, TWEAK or TNF-α did not change levels of apoptosis significantly compared to the untreated control (Figure 9B). Nevertheless a slight increase of apoptosis was detected during the second experiment when cells were treated with TWEAK compared to untreated control (Figure 9B). TNF-α stimulation for 12 hours increased levels of necrosis slightly but not for 24 hours compared to the untreated control. Stimulation of MSC with TWEAK for 12 hours did not seem to have an effect on necrosis but slightly increased levels of necrosis in the second 24 hours experiment. (Figure 9C). Although the changes in histograms have been minor it appears that TWEAK induces cell death considering the low number of cells detected after the second 24 hours experiment.

ROS production was enhanced after 12 hours and the first 24 hours experiment but not the second 24 hours experiment with TNF-α stimulation (Figure 9D). TWEAK stimulation did not change levels of ROS production after 12 hours or the second 24 hours experiment but increased ROS production slightly after the first 24 hours experiment (Figure 9D).

Surprisingly, treatment with TWEAK led to a substantial decrease of autophagy after the second 24 hours experiment compared to unstimulated control and TNF-α (Figure 9E) but could not be repeated after 12 or 24 hours (Figure 9E). TNF-α stimulation slightly enhanced levels of autophagy after 12 hours but not after 24 hours compared to the untreated control (Figure 9E).

Overall, TNF-α stimulation did not seem to affect apoptosis, necrosis, ROS production or autophagy in MSC. In addition, TWEAK stimulation did not have a great impact on levels of apoptosis, necrosis and ROS production except on levels of autophagy and cell death in one experiment after 24-hour stimulation (Figure 9, 2: 24 hours).

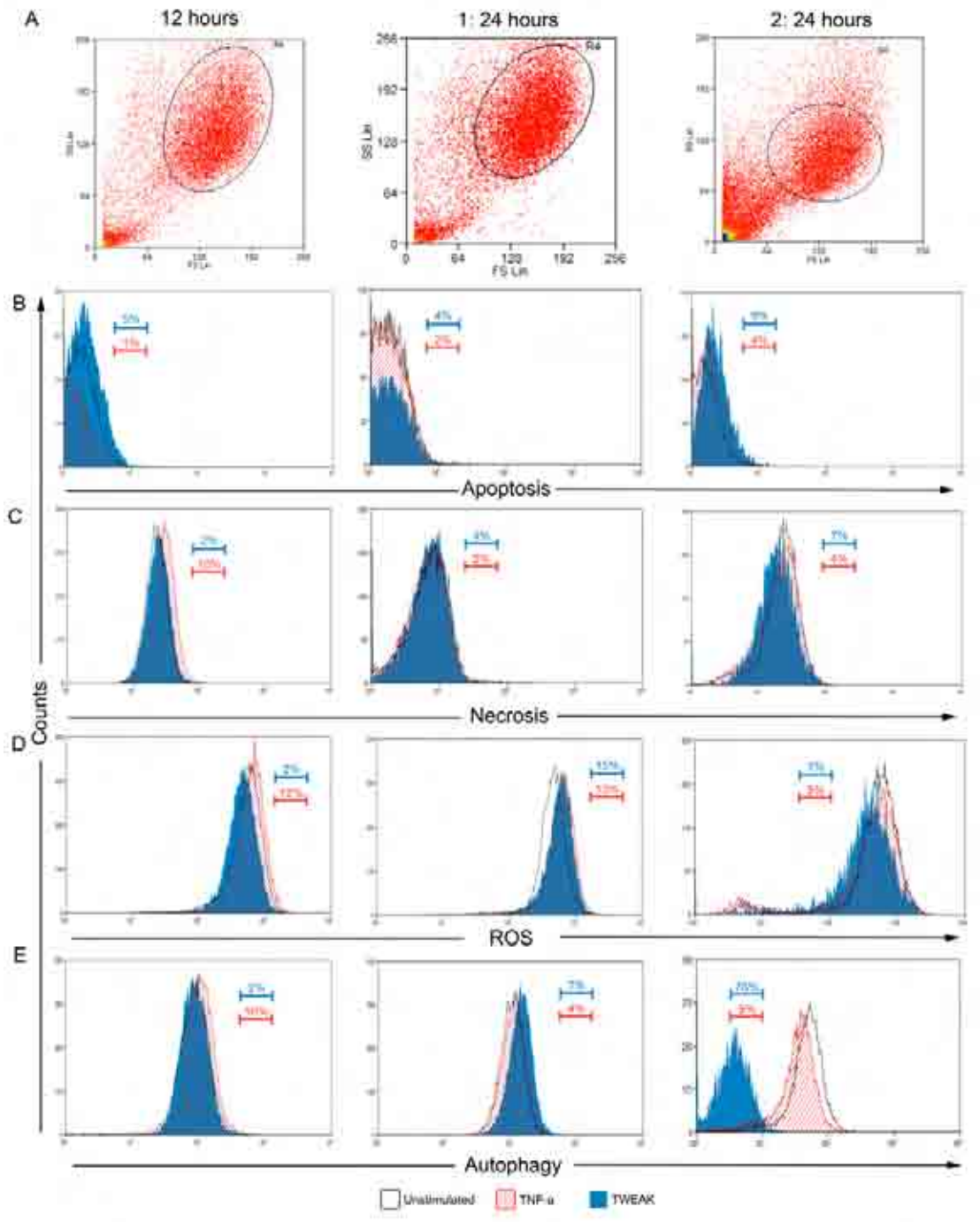

Fig 9. Flow cytometric analysis of apoptosis, necrosis, ROS production and autophagy in MSC. MSC were stimulated for 12 or 24 hours with TWEAK or TNF-α. Forward versus side scatter with at least 10,000 gated events after 12, first 24 or second 24 hours (A) Flow cytometry analysis was carried out for apoptosis (B) necrosis (C) ROS production (D) and autophagy (E). Presented data is for individual experiments.

4.7 Fn14 Expression on HSC

Since there is no published data regarding Fn14 expression on HSC, Fn14 expression was investigated with flow cytometry and immunocytochemistry on unstimulated and TGF-β stimulated HSC. HSC have a star-like morphology (Figure 10A) but when they are treated with TGF-β they become activated and form clusters (116) (Figure 10B). Flow cytometry analysis showed that 83% of unstimulated HSC and 89% of TGF-β stimulated HSC expressed Fn14 (Figure 10C).

The MFI of Fn14 in unstimulated HSC is 38 but it significantly increases to 49 (p= < 0.05) when HSC were stimulated with TGF-β. Fn14 expression was confirmed with immunocytochemistry on unstimulated and TGF- β stimulated HSC (Figure 10D).

Overall, there has been in an increase in MFI and Fn14 expressing HSC when they were stimulated with TGF-β.

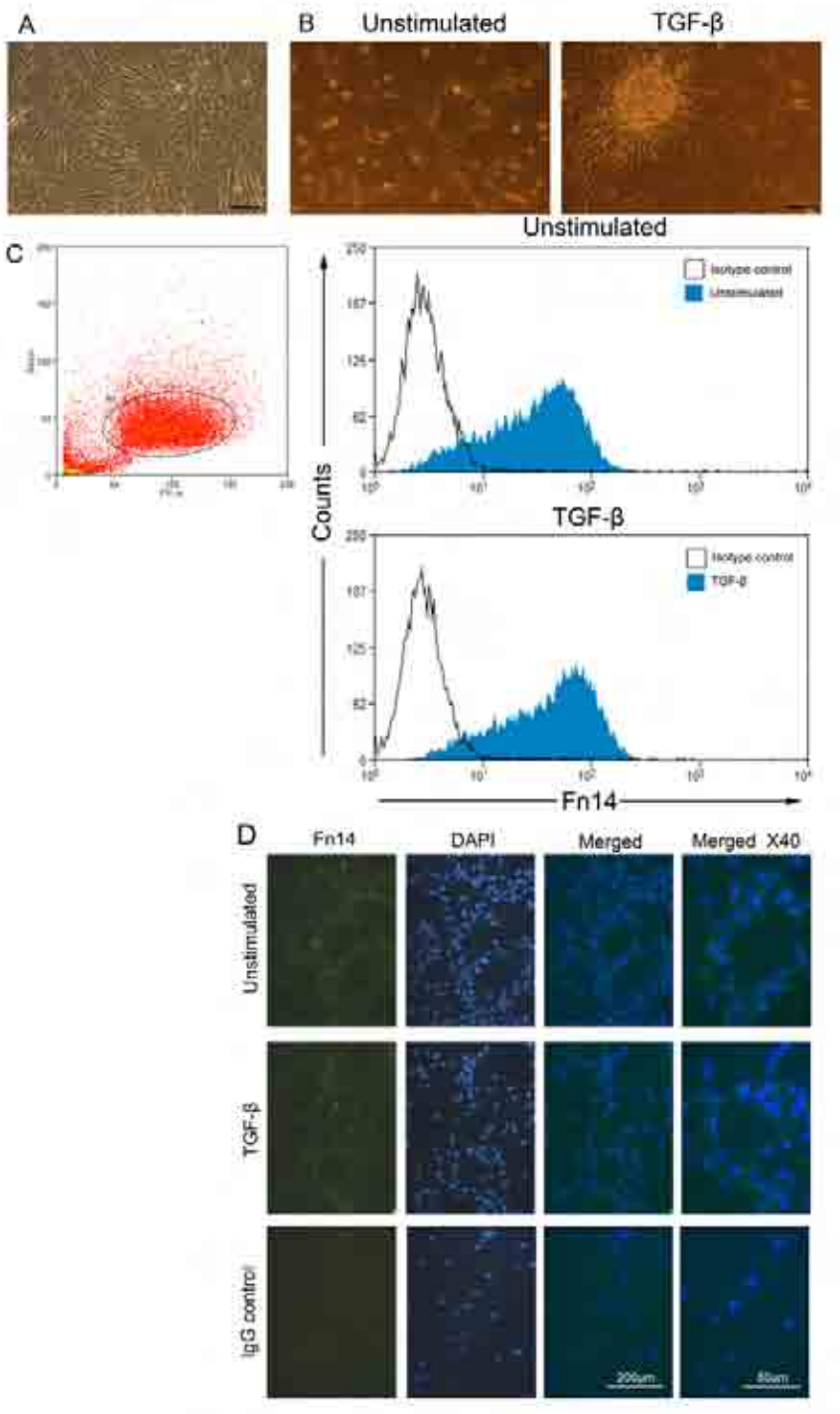

Fig 10. Fn14 expression on HSC Morphology of HSC (A) Morphology of TGF-β stimulated HSC compared to unstimulated HSC (B) Flow cytometric analysis of Fn14 expression on unstimulated and TGF-β stimulated HSC (C) Unstimulated and TGF-β stimulated HSC positive for Fn14 expression counterstained with DAPI. Scale bar, 200μm. Scale bar merged X40 50μm (D)

5. DISCUSSION

Currently the only effective treatment for cirrhosis is liver transplantation. However, the lack of available organs and the fact that transplant patients have to take lifelong toxic immunosuppressive medications leads to a need to discover novel treatments. Cellular therapies using stem cells such as MSC provide a promising approach. MSC are easy to isolate and cultivate, can modulate the immune system and can differentiate into hepatocytes. Another possible therapeutic approach would be to reduce the number of ECM producing myofibroblasts within the liver. HSC are the main cell type to give rise to myofibroblast when they become activated during liver injury. Therefore, inhibiting HSC activation or causing apoptosis provide another possible approach to reduce liver fibrosis.

It has been demonstrated that TWEAK-dependent Fn14 signalling is involved in stimulating properties of MSC including activation of pro-survival, pro-proliferative and cell adhesion genes (110). Fn14 expression is very low on hepatocytes in normal livers but becomes highly up-regulated on hepatocytes during liver regeneration (108). In addition, TWEAK is highly expressed by immunocytes and has been detected in tissues with acute injury and inflammation (95,96). Being able to understand how TWEAK-dependent Fn14 signalling affects MSC during transplantation into a fibrotic liver would be a major advantage for cell therapy. It has been demonstrated that MSC can differentiate into myofibroblasts (90). Therefore it would be beneficial to look at

the effect of TWEAK on MSC differentiation in order to advance to safe cell therapy. Also, to understand how TWEAK-dependent Fn14 signalling might affect HSC activation during fibrosis may provide us with another avenue for therapeutic intervention.

5.1 Expression of TWEAK and Fn14 on MSC

MSC used for this project were heterogeneous in size and displayed a fibroblast like morphology. They expressed the surface markers CD73, CD90 and CD105 and were negative for the haematopoietic markers CD34 and CD45, the B cell marker CD20 and the monocyte/macrophage marker CD14. One study has demonstrated that MSC express Fn14 (110). Carrying out flow cytometry on unstimulated MSC confirmed these findings.

As mentioned above, TWEAK, TNF-α and their receptors are part of the same superfamily. MSC respond to TNF-α stimulation in a number of ways such as enhanced cell migration, proliferation (92), adhesion (unpublished data from V. Aldridge) and increased immunosuppressive abilities (80). In addition, bone marrow derived MSC have been demonstrated to respond to TNF-α stimulation causing NF-κB translocation (117). To investigate the effect of TNF-α on Fn14 expression on MSC, we treated MSC with TNF-α for 24 hours. Treatment did not seem to affect the number of cells expressing Fn14 but it increased the MFI, which indicates that more Fn14 receptors were expressed per cell. This suggests that TNF-α makes MSC more susceptible to stimulation with TWEAK by inducing increased expression of Fn14. Immunocytochemistry confirmed that unstimulated and TNF-α stimulated MSC expressed Fn14.

It has not previously been reported whether MSC express TWEAK. Flow cytometry analysis showed that MSC did not express TWEAK on the cell surface or intracellular. This suggests that Fn14 signalling in MSC is not affected by autocrine action.

5.2 Fn14 Expression during Adipogenesis

As MSC highly express Fn14, we were interested to see whether MSC loose Fn14 expression during differentiation. Therefore, MSC were differentiated with an adipogenic differentiation kit and analysed after every cycle for Fn14 expression. Flow cytometric analysis shows that Fn14 expression on MSC decreased steadily during adipogenesis. These results are in accordance with data published by Alexaki *et al*. who demonstrated that Fn14 expression decreases when adipose tissue derived mesenchymal cells (ADMC) or MSC undergo adipogenesis (111). They also showed that Fn14 translocates from the cell surface to inside the cell during adipogenic differentiation of ADMC (111). This could explain why the MFI drops after cycle 3 during adipogenesis of MSC. However, the expression of Fn14 is not completely lost and this may be explained by the fact that Fn14 is still expressed at low levels in adipose tissue (111). Furthermore, some undifferentiated cells remained within the adipogenic culture, therefore these cells may still express high levels of Fn14. A way of deciphering whether Fn14 expression is lost on our adipocytes would be to include an adipocyte-specific antibody in our flow cytometry analysis.

Surprisingly, Fn14 expression also decreased in both control media. The cells remained MSC and kept on differentiating resulting in more cells per well. This

suggests that expression levels of Fn14 might be influenced by confluency. The maintenance medium decreased the number of MSC expressing Fn14 more than the MSC medium alone, suggesting it may contain factors not found in the MSC medium. Since we obtain the media commercially we are unable to determine whether there are any factors in the maintenance medium, which would affect Fn14 expression.

5.3 Effect of TWEAK during Adipogenesis

Corresponding to the decreasing levels of Fn14 during adipogenesis, TWEAK is present in immature adipose tissue but not in fully differentiated adipose tissue (110). Also, it has been demonstrated that TWEAK decreases adipogenic differentiation of ADMC (110). Treating MSC with TWEAK protein during adipogenesis did not seem to affect the differentiation potential of MSC. Surprisingly, treating MSC with maintenance medium and TWEAK appeared to enhance proliferation of MSC compared to treatment with maintenance medium alone. Low concentrations of TWEAK (2-10ng/ml) have been associated with increased proliferation of the Eph4 mammary epithelial cell line (118) whereas relatively high doses of TWEAK (100ng/ml) have been associated with cell death (118). For this experiment low doses of TWEAK (10ng/ml) seemed to induce proliferation, which would correlate with previous research.

5.4 Effect of TWEAK on Apoptosis, Necrosis, ROS Production and Autophagy on MSC

MSC were treated for 12 or 24 hours with either TWEAK, TNF-α or left untreated. Treatment with TWEAK did not change levels of apoptosis in MSC significantly. However, a slight increase in apoptosis was detected in the second 24 hours experiment in which a different batch of TWEAK was used. Therefore it is unclear whether this is a real result or whether there are batch specific effects of TWEAK. More experiments would need to be carried out to address this. However, TWEAK has been reported to induce apoptosis in various cancer cell lines including Kym1 and OVCAR4 (119,120). The mechanisms by which TNF-α and TWEAK have been described to induce apoptosis include activation of transcription factor NF-κB (121), or TWEAK can induce apoptosis by secondary activation of TNF-α (119,120). Other described mechanisms for the action of TWEAK include TNF-α independent but caspase-dependent mechanisms (122). Fewer cells were present to carry out flow cytometry analysis in the second 24 hours experiment compared to the other experiments, which indicates that cells died before the experiment was carried out. This could explain why levels of apoptosis did not increase significantly. Furthermore, it is also possible that TWEAK induced cell death in MSC *via* necrosis rather than apoptosis, as TWEAK has been reported to induce necrosis by reactive oxygen intermediates and cathepsin B-dependent pathways (122).

It has been demonstrated that apoptosis and necrosis can lead to an increase in ROS production resulting in oxidative stress (122). A slight increase of ROS production and necrosis was detected after 12 hours of stimulation with TNF-α. This is in accordance with other published data that demonstrates that TNF-α can induce necrosis, which seems to be mediated by production in ROS (123). In addition, TWEAK stimulation led to an increase in ROS production in the first 24 hours experiment. It has been demonstrated that TWEAK can induce apoptosis through an increase in ROS production in 15d-PGJ_2 sensitized cancer cells (124). This could suggest that cells with increased levels of ROS were about to undergo apoptosis.

Autophagy is also involved in cell death and survival. During autophagy an autophagosome is formed that removes parts of the cytoplasm to either promote or prevent cell death (125). TNF-α stimulation caused a slight increase of autophagy after 12 hours but not after 24 hours. As necrosis and ROS production after 12 hours of TNF-α stimulation was also elevated an increase in autophagy could suggest that cells used autophagy to prevent cell death.

The first batch of TWEAK did not change levels of autophagy after 12 or 24 hours whereas the second batch of TWEAK decreased autophagy significantly compared to TNF-α and untreated control. It has been demonstrated that TWEAK can activate autophagy in cultured myotubes by increasing expression of autophagy-related molecules (126). This indicates that TWEAK can affect autophagy and it is possible that TWEAK might have an inhibitory effect on an autophagy related molecule in MSC, thereby inhibiting autophagy in this

specialised cell type. Alternatively, the remaining cells that have not already undergone cell death may have started to “commit” to death and therefore inactivated autophagy.

5.5 Expression of Fn14 on HSC

HSC play an important role during fibrogenesis and understanding how they are affected by their microenvironment would provide a crucial clue in the treatment of fibrosis. TWEAK has been detected in chronic liver injury (106) and TWEAK-dependent Fn14 signalling can regulate several cellular processes including proliferation and differentiation (100). Therefore it might modulate HSC proliferation or influence differentiation of HSC into myofibroblasts. It would be a great progress to understand how TWEAK-dependent Fn14 signalling might affect HSC during fibrosis.

We have demonstrated for the first time that a high number of unstimulated HSC express Fn14. To activate HSC, they were stimulated with TGF-β for 24 hours and subsequent flow cytometric analysis was carried out for Fn14 expression. It demonstrated that Fn14 expression was slightly increased compared to the untreated control. Furthermore, the MFI significantly increased when HSC were treated with TGF-β compared to untreated cells. This suggests that TGF-β stimulation makes HSC more susceptible to stimulation with TWEAK by increasing the levels of Fn14 expression. In addition, it was not determined whether TGF-β stimulation activated all HSC and the percentage of active HSC expressing Fn14. Examining the co-expression of Fn14 and α-SMA, which is a marker of activated HSC, could test this.

5.6 Future Experiments

Fn14 expression decreased during adipogenesis but both control media also showed lower expression levels of Fn14. Therefore, it is not conclusive whether decreased levels of Fn14 were caused by MSC differentiation or by confluence. Using an adipocyte marker in addition to an Fn14 antibody could determine to what level adipocytes and the undifferentiated MSC express Fn14. In addition, Fn14 expression could be tested on MSC that have been plated at different densities starting from few cells to 100% confluence to test the affect of confluence on Fn14 expression.

TWEAK did not affect adipogenic differentiation of MSC but seem to enhance proliferation. TWEAK has been demonstrated to enhance proliferation in liver progenitor cells (106). Therefore, it would be interesting to see whether TWEAK also enhances proliferation in MSC. To further investigate the effect of TWEAK on cell proliferation, MSC could be treated with TWEAK and proliferation could be quantified with a 5-bromo-2-deoxyuridine (BrdU) assay, 3-(4,5-dimethylthiazol-2-yl)-2,5-diphenyltetrazolium (MTT) assay or the Cellscreen system.

The effect of TWEAK on apoptosis, necrosis, ROS production and autophagy in MSC is inconclusive as different batches of TWEAK show different results. More experiments need to be carried out with both batches of TWEAK. To determine whether TWEAK affects MSC survival, live cells could be quantified with trypan blue staining. Furthermore, terminal deoxynucleotidyl transferase-mediated biotinylated UTP nick end labeling (TUNEL) staining could be used to detect dead cells.

One donor has been used to show that HSC express Fn14. More donors are needed to confirm these results. TWEAK could be used to stimulate HSC with or without TGF-β to see the effect on HSC. In addition α-SMA staining needs to be carried out to assure that HSC have been activated. It would also be interesting to see whether TWEAK changes levels of apoptosis, necrosis, ROS production or autophagy in HSC.

6. REFEERENCES

(1) Ramón y Cajal S, .1852-1934. [Estudios sobre la degeneracio\0301n y regeneracio\0301n del sistema nervioso.] Degeneration & Regeneration of the Nervous System ... Translated and edited by Raoul M. May. [With a portrait.]. 2 vol. pp. xx. viii. 769. Humphrey Milford: London; 1928.

(2) Berkelaar M, Clarke DB, Wang YC, Bray GM, Aguayo AJ. Axotomy results in delayed death and apoptosis of retinal ganglion cells in adult rats. J Neurosci 1994 Jul;14(7):4368-4374.

(3) Troy CM, Ribe EM. Caspase-2: vestigial remnant or master regulator? Sci Signal 2008 Sep 23;1(38):pe42.

(4) Ahmed Z, Kalinski H, Berry M, Almasieh M, Ashush H, Slager N, et al. Ocular neuroprotection by siRNA targeting caspase-2. Cell Death Dis 2011 Jun 16;2:e173.

(5) Kermer P, Klocker N, Labes M, Bahr M. Inhibition of CPP32-like proteases rescues axotomized retinal ganglion cells from secondary cell death in vivo. J Neurosci 1998 Jun 15;18(12):4656-4662.

(6) Bonfanti L, Strettoi E, Chierzi S, Cenni MC, Liu XH, Martinou J-, et al. Protection of retinal ganglion cells from natural and axotomy-induced cell death in neonatal transgenic mice overexpressing bcl-2. J Neurosci 1996 Jul 1;16(13):4186-4194.

(7) Chierzi S, Strettoi E, Cenni MC, Maffei L. Optic nerve crush: axonal responses in wild-type and bcl-2 transgenic mice. J Neurosci 1999 Oct 1;19(19):8367-8376.

(8) Villegas-Perez MP, Vidal-Sanz M, Rasminsky M, Bray GM, Aguayo AJ. Rapid and protracted phases of retinal ganglion cell loss follow axotomy in the optic nerve of adult rats. J Neurobiol 1993 Jan;24(1):23-36.

(9) Caroni P, Savio T, Schwab ME. Central nervous system regeneration: oligodendrocytes and myelin as non-permissive substrates for neurite growth. Prog Brain Res 1988;78:363-370.

(10) Rolls A, Shechter R, Schwartz M. The bright side of the glial scar in CNS repair. Nat Rev Neurosci 2009 Mar;10(3):235-241.
(11) Pizzorusso T, Medini P, Berardi N, Chierzi S, Fawcett JW, Maffei L. Reactivation of ocular dominance plasticity in the adult visual cortex. Science 2002 Nov 8;298(5596):1248-1251.
(12) Chen MS, Huber AB, van der Haar ME, Frank M, Schnell L, Spillmann AA, et al. Nogo-A is a myelin-associated neurite outgrowth inhibitor and an antigen for monoclonal antibody IN-1. Nature 2000 Jan 27;403(6768):434-439.
(13) McKerracher L, David S, Jackson DL, Kottis V, Dunn RJ, Braun PE. Identification of myelin-associated glycoprotein as a major myelin-derived inhibitor of neurite growth. Neuron 1994 Oct;13(4):805-811.
(14) Wang KC, Koprivica V, Kim JA, Sivasankaran R, Guo Y, Neve RL, et al. Oligodendrocyte-myelin glycoprotein is a Nogo receptor ligand that inhibits neurite outgrowth. Nature 2002 Jun 27;417(6892):941-944.
(15) Mi S, Lee X, Shao Z, Thill G, Ji B, Relton J, et al. LINGO-1 is a component of the Nogo-66 receptor/p75 signaling complex. Nat Neurosci 2004 Mar;7(3):221-228.
(16) Wang KC, Kim JA, Sivasankaran R, Segal R, He Z. P75 interacts with the Nogo receptor as a co-receptor for Nogo, MAG and OMgp. Nature 2002 Nov 7;420(6911):74-78.
(17) Park JB, Yiu G, Kaneko S, Wang J, Chang J, He XL, et al. A TNF receptor family member, TROY, is a coreceptor with Nogo receptor in mediating the inhibitory activity of myelin inhibitors. Neuron 2005 Feb 3;45(3):345-351.
(18) Wong ST, Henley JR, Kanning KC, Huang KH, Bothwell M, Poo MM. A p75(NTR) and Nogo receptor complex mediates repulsive signaling by myelin-associated glycoprotein. Nat Neurosci 2002 Dec;5(12):1302-1308.
(19) Thomas R, Favell K, Morante-Redolat J, Pool M, Kent C, Wright M, et al. LGI1 is a Nogo receptor 1 ligand that antagonizes myelin-based growth inhibition. J Neurosci 2010 May 12;30(19):6607-6612.
(20) Grunewald E, Kinnell HL, Porteous DJ, Thomson PA. GPR50 interacts with neuronal NOGO-A and affects neurite outgrowth. Mol Cell Neurosci 2009 Dec;42(4):363-371.

(21) Silver J, Miller JH. Regeneration beyond the glial scar. Nat Rev Neurosci 2004 Feb;5(2):146-156.
(22) Shen Y, Tenney AP, Busch SA, Horn KP, Cuascut FX, Liu K, et al. PTPsigma is a receptor for chondroitin sulfate proteoglycan, an inhibitor of neural regeneration. Science 2009 Oct 23;326(5952):592-596.
(23) Fischer D, He Z, Benowitz LI. Counteracting the Nogo receptor enhances optic nerve regeneration if retinal ganglion cells are in an active growth state. J Neurosci 2004 Feb 18;24(7):1646-1651.
(24) Woolf CJ. No Nogo: now where to go? Neuron 2003 Apr 24;38(2):153-156.
(25) Ng TF, So KF, Chung SK. Influence of peripheral nerve grafts on the expression of GAP-43 in regenerating retinal ganglion cells in adult hamsters. J Neurocytol 1995 Jul;24(7):487-496.
(26) Berry M, Carlile J, Hunter A. Peripheral nerve explants grafted into the vitreous body of the eye promote the regeneration of retinal ganglion cell axons severed in the optic nerve. J Neurocytol 1996 Feb;25(2):147-170.
(27) Leon S, Yin Y, Nguyen J, Irwin N, Benowitz LI. Lens injury stimulates axon regeneration in the mature rat optic nerve. J Neurosci 2000 Jun 15;20(12):4615-4626.
(28) Fischer D, Heiduschka P, Thanos S. Lens-injury-stimulated axonal regeneration throughout the optic pathway of adult rats. Exp Neurol 2001 Dec;172(2):257-272.
(29) Yin Y, Cui Q, Li Y, Irwin N, Fischer D, Harvey AR, et al. Macrophage-derived factors stimulate optic nerve regeneration. J Neurosci 2003 Mar 15;23(6):2284-2293.
(30) Yin Y, Henzl MT, Lorber B, Nakazawa T, Thomas TT, Jiang F, et al. Oncomodulin is a macrophage-derived signal for axon regeneration in retinal ganglion cells. Nat Neurosci 2006 Jun;9(6):843-852.
(31) Yin Y, Cui Q, Gilbert HY, Yang Y, Yang Z, Berlinicke C, et al. Oncomodulin links inflammation to optic nerve regeneration. Proc Natl Acad Sci U S A 2009 Nov 17;106(46):19587-19592.
(32) Kurimoto T, Yin Y, Omura K, Gilbert HY, Kim D, Cen LP, et al. Long-distance axon regeneration in the mature optic nerve: contributions of

oncomodulin, cAMP, and pten gene deletion. J Neurosci 2010 Nov 17;30(46):15654-15663.
(33) Leaver SG, Cui Q, Plant GW, Arulpragasam A, Hisheh S, Verhaagen J, et al. AAV-mediated expression of CNTF promotes long-term survival and regeneration of adult rat retinal ganglion cells. Gene Ther 2006 Sep;13(18):1328-1341.
(34) Logan A, Ahmed Z, Baird A, Gonzalez AM, Berry M. Neurotrophic factor synergy is required for neuronal survival and disinhibited axon regeneration after CNS injury. Brain 2006 Feb;129(Pt 2):490-502.
(35) Manning BD. Balancing Akt with S6K: implications for both metabolic diseases and tumorigenesis. J Cell Biol 2004 Nov 8;167(3):399-403.
(36) Pan D, Dong J, Zhang Y, Gao X. Tuberous sclerosis complex: from Drosophila to human disease. Trends Cell Biol 2004 Feb;14(2):78-85.
(37) Brugarolas J, Lei K, Hurley RL, Manning BD, Reiling JH, Hafen E, et al. Regulation of mTOR function in response to hypoxia by REDD1 and the TSC1/TSC2 tumor suppressor complex. Genes Dev 2004 Dec 1;18(23):2893-2904.
(38) Park KK, Liu K, Hu Y, Kanter JL, He Z. PTEN/mTOR and axon regeneration. Exp Neurol 2010 May;223(1):45-50.
(39) Corradetti MN, Inoki K, Guan KL. The stress-inducted proteins RTP801 and RTP801L are negative regulators of the mammalian target of rapamycin pathway. J Biol Chem 2005 Mar 18;280(11):9769-9772.
(40) Ma XM, Blenis J. Molecular mechanisms of mTOR-mediated translational control. Nat Rev Mol Cell Biol 2009 May;10(5):307-318.
(41) Park KK, Liu K, Hu Y, Smith PD, Wang C, Cai B, et al. Promoting axon regeneration in the adult CNS by modulation of the PTEN/mTOR pathway. Science 2008 Nov 7;322(5903):963-966.
(42) Tapon N, Ito N, Dickson BJ, Treisman JE, Hariharan IK. The Drosophila tuberous sclerosis complex gene homologs restrict cell growth and cell proliferation. Cell 2001 May 4;105(3):345-355.
(43) Inoki K, Li Y, Zhu T, Wu J, Guan KL. TSC2 is phosphorylated and inhibited by Akt and suppresses mTOR signalling. Nat Cell Biol 2002 Sep;4(9):648-657.

(44) Choi YJ, Di Nardo A, Kramvis I, Meikle L, Kwiatkowski DJ, Sahin M, et al. Tuberous sclerosis complex proteins control axon formation. Genes Dev 2008 Sep 15;22(18):2485-2495.
(45) DeYoung MP, Horak P, Sofer A, Sgroi D, Ellisen LW. Hypoxia regulates TSC1/2-mTOR signaling and tumor suppression through REDD1-mediated 14-3-3 shuttling. Genes Dev 2008 Jan 15;22(2):239-251.
(46) Sofer A, Lei K, Johannessen CM, Ellisen LW. Regulation of mTOR and cell growth in response to energy stress by REDD1. Mol Cell Biol 2005 Jul;25(14):5834-5845.
(47) Shoshani T, Faerman A, Mett I, Zelin E, Tenne T, Gorodin S, et al. Identification of a novel hypoxia-inducible factor 1-responsive gene, RTP801, involved in apoptosis. Mol Cell Biol 2002 Apr;22(7):2283-2293.
(48) Ellisen LW, Ramsayer KD, Johannessen CM, Yang A, Beppu H, Minda K, et al. REDD1, a developmentally regulated transcriptional target of p63 and p53, links p63 to regulation of reactive oxygen species. Mol Cell 2002 Nov;10(5):995-1005.
(49) Malagelada C, Jin ZH, Greene LA. RTP801 is induced in Parkinson's disease and mediates neuron death by inhibiting Akt phosphorylation/activation. J Neurosci 2008 Dec 31;28(53):14363-14371.
(50) Brafman A, Mett I, Shafir M, Gottlieb H, Damari G, Gozlan-Kelner S, et al. Inhibition of oxygen-induced retinopathy in RTP801-deficient mice. Invest Ophthalmol Vis Sci 2004 Oct;45(10):3796-3805.
(51) Malagelada C, Lopez-Toledano MA, Willett RT, Jin ZH, Shelanski ML, Greene LA. RTP801/REDD1 regulates the timing of cortical neurogenesis and neuron migration. J Neurosci 2011 Mar 2;31(9):3186-3196.
(52) Bantounas I, Phylactou LA, Uney JB. RNA interference and the use of small interfering RNA to study gene function in mammalian systems. J Mol Endocrinol 2004 Dec;33(3):545-557.
(53) Provost P, Dishart D, Doucet J, Frendewey D, Samuelsson B, Radmark O. Ribonuclease activity and RNA binding of recombinant human Dicer. EMBO J 2002 Nov 1;21(21):5864-5874.

(54) Elbashir SM, Harborth J, Lendeckel W, Yalcin A, Weber K, Tuschl T. Duplexes of 21-nucleotide RNAs mediate RNA interference in cultured mammalian cells. Nature 2001 May 24;411(6836):494-498.
(55) Gonzalez-Alegre P. Therapeutic RNA interference for neurodegenerative diseases]. Rev Neurol 2008 Dec 16-31;47(12):641-647.
(56) Oyesiku NM, Wigston DJ. Ciliary neurotrophic factor stimulates neurite outgrowth from spinal cord neurons. J Comp Neurol 1996 Jan 1;364(1):68-77.
(57) Bataller R, Brenner DA. Liver fibrosis. J Clin Invest 2005 Feb;115(2):209-218.
(58) Brown B, Lindberg K, Reing J, Stolz DB, Badylak SF. The basement membrane component of biologic scaffolds derived from extracellular matrix. Tissue Eng 2006 Mar;12(3):519-526.
(59) Blomhoff R, Wake K. Perisinusoidal stellate cells of the liver: important roles in retinol metabolism and fibrosis. FASEB J 1991 Mar 1;5(3):271-277.
(60) Milani S, Herbst H, Schuppan D, Kim KY, Riecken EO, Stein H. Procollagen expression by nonparenchymal rat liver cells in experimental biliary fibrosis. Gastroenterology 1990 Jan;98(1):175-184.
(61) Marra F. Hepatic stellate cells and the regulation of liver inflammation. J Hepatol 1999 Dec;31(6):1120-1130.
(62) Gressner AM, Weiskirchen R, Breitkopf K, Dooley S. Roles of TGF-beta in hepatic fibrosis. Front Biosci 2002 Apr 1;7:d793-807.
(63) Shek FW, Benyon RC. How can transforming growth factor beta be targeted usefully to combat liver fibrosis? Eur J Gastroenterol Hepatol 2004 Feb;16(2):123-126.
(64) Beaussier M, Wendum D, Schiffer E, Dumont S, Rey C, Lienhart A, et al. Prominent contribution of portal mesenchymal cells to liver fibrosis in ischemic and obstructive cholestatic injuries. Lab Invest 2007 Mar;87(3):292-303.
(65) Kisseleva T, Uchinami H, Feirt N, Quintana-Bustamante O, Segovia JC, Schwabe RF, et al. Bone marrow-derived fibrocytes participate in pathogenesis of liver fibrosis. J Hepatol 2006 Sep;45(3):429-438.

(66) Forbes SJ, Russo FP, Rey V, Burra P, Rugge M, Wright NA, et al. A significant proportion of myofibroblasts are of bone marrow origin in human liver fibrosis. Gastroenterology 2004 Apr;126(4):955-963.
(67) Zeisberg M, Yang C, Martino M, Duncan MB, Rieder F, Tanjore H, et al. Fibroblasts derive from hepatocytes in liver fibrosis via epithelial to mesenchymal transition. J Biol Chem 2007 Aug 10;282(32):23337-23347.
(68) Moreira RK. Hepatic stellate cells and liver fibrosis. Arch Pathol Lab Med 2007 Nov;131(11):1728-1734.
(69) Friedman SL. Mechanisms of hepatic fibrogenesis. Gastroenterology 2008 May;134(6):1655-1669.
(70) Arthur MJ. Reversibility of liver fibrosis and cirrhosis following treatment for hepatitis C. Gastroenterology 2002 May;122(5):1525-1528.
(71) Pares A, Caballeria J, Bruguera M, Torres M, Rodes J. Histological course of alcoholic hepatitis. Influence of abstinence, sex and extent of hepatic damage. J Hepatol 1986;2(1):33-42.
(72) Kharaziha P, Hellstrom PM, Noorinayer B, Farzaneh F, Aghajani K, Jafari F, et al. Improvement of liver function in liver cirrhosis patients after autologous mesenchymal stem cell injection: a phase I-II clinical trial. Eur J Gastroenterol Hepatol 2009 Oct;21(10):1199-1205.
(73) Pai M, Zacharoulis D, Milicevic MN, Helmy S, Jiao LR, Levicar N, et al. Autologous infusion of expanded mobilized adult bone marrow-derived CD34+ cells into patients with alcoholic liver cirrhosis. Am J Gastroenterol 2008 Aug;103(8):1952-1958.
(74) Terai S, Ishikawa T, Omori K, Aoyama K, Marumoto Y, Urata Y, et al. Improved liver function in patients with liver cirrhosis after autologous bone marrow cell infusion therapy. Stem Cells 2006 Oct;24(10):2292-2298.
(75) Parekkadan B, van Poll D, Megeed Z, Kobayashi N, Tilles AW, Berthiaume F, et al. Immunomodulation of activated hepatic stellate cells by mesenchymal stem cells. Biochem Biophys Res Commun 2007 Nov 16;363(2):247-252.
(76) Le Blanc K, Ringden O. Mesenchymal stem cells: properties and role in clinical bone marrow transplantation. Curr Opin Immunol 2006 Oct;18(5):586-591.

(77) Schraufstatter IU, Discipio RG, Khaldoyanidi S. Mesenchymal stem cells and their microenvironment. Front Biosci 2011 Jun 1;17:2271-2288.
(78) Ortiz LA, Dutreil M, Fattman C, Pandey AC, Torres G, Go K, et al. Interleukin 1 receptor antagonist mediates the antiinflammatory and antifibrotic effect of mesenchymal stem cells during lung injury. Proc Natl Acad Sci U S A 2007 Jun 26;104(26):11002-11007.
(79) Ren G, Zhang L, Zhao X, Xu G, Zhang Y, Roberts AI, et al. Mesenchymal stem cell-mediated immunosuppression occurs via concerted action of chemokines and nitric oxide. Cell Stem Cell 2008 Feb 7;2(2):141-150.
(80) Shi Y, Hu G, Su J, Li W, Chen Q, Shou P, et al. Mesenchymal stem cells: a new strategy for immunosuppression and tissue repair. Cell Res 2010 May;20(5):510-518.
(81) Tse WT, Pendleton JD, Beyer WM, Egalka MC, Guinan EC. Suppression of allogeneic T-cell proliferation by human marrow stromal cells: implications in transplantation. Transplantation 2003 Feb 15;75(3):389-397.
(82) Jiang Y, Jahagirdar BN, Reinhardt RL, Schwartz RE, Keene CD, Ortiz-Gonzalez XR, et al. Pluripotency of mesenchymal stem cells derived from adult marrow. Nature 2002 Jul 4;418(6893):41-49.
(83) Schwartz RE, Reyes M, Koodie L, Jiang Y, Blackstad M, Lund T, et al. Multipotent adult progenitor cells from bone marrow differentiate into functional hepatocyte-like cells. J Clin Invest 2002 May;109(10):1291-1302.
(84) Korbling M, Katz RL, Khanna A, Ruifrok AC, Rondon G, Albitar M, et al. Hepatocytes and epithelial cells of donor origin in recipients of peripheral-blood stem cells. N Engl J Med 2002 Mar 7;346(10):738-746.
(85) di Bonzo LV, Ferrero I, Cravanzola C, Mareschi K, Rustichell D, Novo E, et al. Human mesenchymal stem cells as a two-edged sword in hepatic regenerative medicine: engraftment and hepatocyte differentiation versus profibrogenic potential. Gut 2008 Feb;57(2):223-231.
(86) van Poll D, Parekkadan B, Cho CH, Berthiaume F, Nahmias Y, Tilles AW, et al. Mesenchymal stem cell-derived molecules directly modulate hepatocellular death and regeneration in vitro and in vivo. Hepatology 2008 May;47(5):1634-1643.

(87) Fang B, Shi M, Liao L, Yang S, Liu Y, Zhao RC. Systemic infusion of FLK1(+) mesenchymal stem cells ameliorate carbon tetrachloride-induced liver fibrosis in mice. Transplantation 2004 Jul 15;78(1):83-88.
(88) Mohamadnejad M, Alimoghaddam K, Mohyeddin-Bonab M, Bagheri M, Bashtar M, Ghanaati H, et al. Phase 1 trial of autologous bone marrow mesenchymal stem cell transplantation in patients with decompensated liver cirrhosis. Arch Iran Med 2007 Oct;10(4):459-466.
(89) Zhao DC, Lei JX, Chen R, Yu WH, Zhang XM, Li SN, et al. Bone marrow-derived mesenchymal stem cells protect against experimental liver fibrosis in rats. World J Gastroenterol 2005 Jun 14;11(22):3431-3440.
(90) Russo FP, Alison MR, Bigger BW, Amofah E, Florou A, Amin F, et al. The bone marrow functionally contributes to liver fibrosis. Gastroenterology 2006 May;130(6):1807-1821.
(91) Bonizzi G, Karin M. The two NF-kappaB activation pathways and their role in innate and adaptive immunity. Trends Immunol 2004 Jun;25(6):280-288.
(92) Bocker W, Docheva D, Prall WC, Egea V, Pappou E, Rossmann O, et al. IKK-2 is required for TNF-alpha-induced invasion and proliferation of human mesenchymal stem cells. J Mol Med (Berl) 2008 Oct;86(10):1183-1192.
(93) Tomita K, Tamiya G, Ando S, Ohsumi K, Chiyo T, Mizutani A, et al. Tumour necrosis factor alpha signalling through activation of Kupffer cells plays an essential role in liver fibrosis of non-alcoholic steatohepatitis in mice. Gut 2006 Mar;55(3):415-424.
(94) Chicheportiche Y, Bourdon PR, Xu H, Hsu YM, Scott H, Hession C, et al. TWEAK, a new secreted ligand in the tumor necrosis factor family that weakly induces apoptosis. J Biol Chem 1997 Dec 19;272(51):32401-32410.
(95) Serafini B, Magliozzi R, Rosicarelli B, Reynolds R, Zheng TS, Aloisi F. Expression of TWEAK and its receptor Fn14 in the multiple sclerosis brain: implications for inflammatory tissue injury. J Neuropathol Exp Neurol 2008 Dec;67(12):1137-1148.
(96) van Kuijk AW, Wijbrandts CA, Vinkenoog M, Zheng TS, Reedquist KA, Tak PP. TWEAK and its receptor Fn14 in the synovium of patients with rheumatoid

arthritis compared to psoriatic arthritis and its response to tumour necrosis factor blockade. Ann Rheum Dis 2010 Jan;69(1):301-304.
(97) Wiley SR, Cassiano L, Lofton T, Davis-Smith T, Winkles JA, Lindner V, et al. A novel TNF receptor family member binds TWEAK and is implicated in angiogenesis. Immunity 2001 Nov;15(5):837-846.
(98) Locksley RM, Killeen N, Lenardo MJ. The TNF and TNF receptor superfamilies: integrating mammalian biology. Cell 2001 Feb 23;104(4):487-501.
(99) Saitoh T, Nakayama M, Nakano H, Yagita H, Yamamoto N, Yamaoka S. TWEAK induces NF-kappaB2 p100 processing and long lasting NF-kappaB activation. J Biol Chem 2003 Sep 19;278(38):36005-36012.
(100) Winkles JA. The TWEAK-Fn14 cytokine-receptor axis: discovery, biology and therapeutic targeting. Nat Rev Drug Discov 2008 May;7(5):411-425.
(101) Jain M, Jakubowski A, Cui L, Shi J, Su L, Bauer M, et al. A novel role for tumor necrosis factor-like weak inducer of apoptosis (TWEAK) in the development of cardiac dysfunction and failure. Circulation 2009 Apr 21;119(15):2058-2068.
(102) Dogra C, Changotra H, Wedhas N, Qin X, Wergedal JE, Kumar A. TNF-related weak inducer of apoptosis (TWEAK) is a potent skeletal muscle-wasting cytokine. FASEB J 2007 Jun;21(8):1857-1869.
(103) Polavarapu R, Gongora MC, Winkles JA, Yepes M. Tumor necrosis factor-like weak inducer of apoptosis increases the permeability of the neurovascular unit through nuclear factor-kappa B pathway activation. J Neurosci 2005 Nov 2;25(44):10094-10100.
(104) Gao HX, Campbell SR, Burkly LC, Jakubowski A, Jarchum I, Banas B, et al. TNF-like weak inducer of apoptosis (TWEAK) induces inflammatory and proliferative effects in human kidney cells. Cytokine 2009 Apr;46(1):24-35.
(105) Zhao Z, Burkly LC, Campbell S, Schwartz N, Molano A, Choudhury A, et al. TWEAK/Fn14 interactions are instrumental in the pathogenesis of nephritis in the chronic graft-versus-host model of systemic lupus erythematosus. J Immunol 2007 Dec 1;179(11):7949-7958.

(106) Tirnitz-Parker JE, Viebahn CS, Jakubowski A, Klopcic BR, Olynyk JK, Yeoh GC, et al. Tumor necrosis factor-like weak inducer of apoptosis is a mitogen for liver progenitor cells. Hepatology 2010 Jul;52(1):291-302.
(107) Jakubowski A, Ambrose C, Parr M, Lincecum JM, Wang MZ, Zheng TS, et al. TWEAK induces liver progenitor cell proliferation. J Clin Invest 2005 Sep;115(9):2330-2340.
(108) Feng SL, Guo Y, Factor VM, Thorgeirsson SS, Bell DW, Testa JR, et al. The Fn14 immediate-early response gene is induced during liver regeneration and highly expressed in both human and murine hepatocellular carcinomas. Am J Pathol 2000 Apr;156(4):1253-1261.
(109) Campbell S, Michaelson J, Burkly L, Putterman C. The role of TWEAK/Fn14 in the pathogenesis of inflammation and systemic autoimmunity. Front Biosci 2004 Sep 1;9:2273-2284.
(110) Girgenrath M, Weng S, Kostek CA, Browning B, Wang M, Brown SA, et al. TWEAK, via its receptor Fn14, is a novel regulator of mesenchymal progenitor cells and skeletal muscle regeneration. EMBO J 2006 Dec 13;25(24):5826-5839.
(111) Alexaki VI, Notas G, Pelekanou V, Kampa M, Valkanou M, Theodoropoulos P, et al. Adipocytes as immune cells: differential expression of TWEAK, BAFF, and APRIL and their receptors (Fn14, BAFF-R, TACI, and BCMA) at different stages of normal and pathological adipose tissue development. J Immunol 2009 Nov 1;183(9):5948-5956.
(112) Myhre O, Andersen JM, Aarnes H, Fonnum F. Evaluation of the probes 2',7'-dichlorofluorescin diacetate, luminol, and lucigenin as indicators of reactive species formation. Biochem Pharmacol 2003 May 15;65(10):1575-1582.
(113) Biederbick A, Kern HF, Elsasser HP. Monodansylcadaverine (MDC) is a specific in vivo marker for autophagic vacuoles. Eur J Cell Biol 1995 Jan;66(1):3-14.
(114) Andree HA, Reutelingsperger CP, Hauptmann R, Hemker HC, Hermens WT, Willems GM. Binding of vascular anticoagulant alpha (VAC alpha) to planar phospholipid bilayers. J Biol Chem 1990 Mar 25;265(9):4923-4928.
(115) Schmid I, Krall WJ, Uittenbogaart CH, Braun J, Giorgi JV. Dead cell discrimination with 7-amino-actinomycin D in combination with dual color

immunofluorescence in single laser flow cytometry. Cytometry 1992;13(2):204-208.
(116) Thomas RJ, Bennett A, Thomson B, Shakesheff KM. Hepatic stellate cells on poly(DL-lactic acid) surfaces control the formation of 3D hepatocyte co-culture aggregates in vitro. Eur Cell Mater 2006 Jan 23;11:16-26; discussion 26.
(117) van den Berk LC, Jansen BJ, Siebers-Vermeulen KG, Roelofs H, Figdor CG, Adema GJ, et al. Mesenchymal stem cells respond to TNF but do not produce TNF. J Leukoc Biol 2010 Feb;87(2):283-289.
(118) Burkly LC, Michaelson JS, Hahm K, Jakubowski A, Zheng TS. TWEAKing tissue remodeling by a multifunctional cytokine: role of TWEAK/Fn14 pathway in health and disease. Cytokine 2007 Oct;40(1):1-16.
(119) Schneider P, Schwenzer R, Haas E, Muhlenbeck F, Schubert G, Scheurich P, et al. TWEAK can induce cell death via endogenous TNF and TNF receptor 1. Eur J Immunol 1999 Jun;29(6):1785-1792.
(120) Vince JE, Chau D, Callus B, Wong WW, Hawkins CJ, Schneider P, et al. TWEAK-FN14 signaling induces lysosomal degradation of a cIAP1-TRAF2 complex to sensitize tumor cells to TNFalpha. J Cell Biol 2008 Jul 14;182(1):171-184.
(121) Gaur U, Aggarwal BB. Regulation of proliferation, survival and apoptosis by members of the TNF superfamily. Biochem Pharmacol 2003 Oct 15;66(8):1403-1408.
(122) Nakayama M, Ishidoh K, Kojima Y, Harada N, Kominami E, Okumura K, et al. Fibroblast growth factor-inducible 14 mediates multiple pathways of TWEAK-induced cell death. J Immunol 2003 Jan 1;170(1):341-348.
(123) Khwaja A, Tatton L. Resistance to the cytotoxic effects of tumor necrosis factor alpha can be overcome by inhibition of a FADD/caspase-dependent signaling pathway. J Biol Chem 1999 Dec 17;274(51):36817-36823.
(124) Dionne S, Levy E, Levesque D, Seidman EG. PPARgamma ligand 15-deoxy-delta 12,14-prostaglandin J2 sensitizes human colon carcinoma cells to TWEAK-induced apoptosis. Anticancer Res 2010 Jan;30(1):157-166.
(125) Levine B, Kroemer G. Autophagy in the pathogenesis of disease. Cell 2008 Jan 11;132(1):27-42.

(126) Bhatnagar S, Mittal A, Gupta SK, Kumar A. TWEAK causes myotube atrophy through coordinated activation of ubiquitin-proteasome system, autophagy, and caspases. J Cell Physiol 2011 May 12.